THE INFLUENCE OF COFACTORS ON THE FLOCCULATION PROPERTIES OF POLYETHYLENE OXIDE

A Thesis

by

Alain Carignan, B.Eng., École Polytechnique de Montréal

Submitted to the Faculty of Graduate Studies
and Research of McGill University in partial
fulfilment to the requirements for the
degree of Master in Engineering

Department of Chemical Engineering
McGill University
Montreal, Quebec, Canada

June, 1996

National Library of Canada

Acquisitions and Bibliographic Services Branch

395 Wellington Street
Ottawa, Ontario
K1A 0N4

Bibliothèque nationale du Canada

Direction des acquisitions et des services bibliographiques

395, rue Wellington
Ottawa (Ontario)
K1A 0N4

Your file Votre référence

Our file Notre référence

ISBN 0-612-19863-4

Je n'en finis plus de découvrir

ces merveilles de la nature

que Dieu a bien voulu nous offrir

ABSTRACT

Higher paper machine speed, efficiency and paper quality like opacity, can be attained by increasing the first-pass retention. Adding polyethylene oxide (PEO) at the wet end of a paper machine, can result in an increase in retention of the fine particles. However, controversy is still surrounding the mechanism by which PEO helps to retain the colloidal particles. The results obtained with PEO and the cofactors (SNS, MPR, and CAR), are discussed in terms of the association-induced polymer bridging mechanism.

Dynamic Light Scattering (DLS) of polymer solutions revealed that each of the three cofactors are forming complexes with PEO. CAR radically increased the apparent diameter of the PEO chains, and MPR seems to decrease it. In latex suspensions, the SNS was found very efficient in the sequence latex-polymer-cofactor (LPC), increasing the PEO hydrodynamic layer thickness (HLT). A thermodynamic equilibrium seems to take place at a HLT of about 40 nm.

Flocculation experiments with the help of a Photometric Dispersion Analyser (PDA), with PEO only (no cofactor) suggested that the fines are composed of more than one component. SNS was found to make all the fines alike by adsorbing on them. Adding the PEO after SNS gave homoflocculation. As a result, the specific surface of fines, calculated by PEO adsorption was found to be 0.223 m^2/g.

The association-induced polymer bridging mechanism can happen in three different manners depending if the cofactor and the polymer are adsorbing onto fines. When neither of PEO nor cofactor adsorb onto the collector, the PEO/cofactor association-complexes bridge the particles (van de Ven and Alince (1996)). When the cofactor (e.g. SNS) and the polymer adsorb onto the fines, in the sequence fines-cofactor-polymer (FCP), with a

chemical ratio cofactor : PEO of 3 : 1, adsorption of the PEO chains onto cofactor-coated fines is likely to occur at the beginning followed by the flocculation of the fines. In the sequence fines-polymer-cofactor (FPC), when the polymer adsorbs onto the fines and the cofactor adsorbs (e.g. SNS) or not (e.g. MPR), a reenforcement of the bondstrength was noticed. This could be caused by the bridging of PEO-coated fines by the cofactor.

RÉSUMÉ

L'augmentation de la vitesse d'une machine à papier, son efficacité et l'opacité du papier peuvent être augmentés en améliorant la rétention de première passe. L'addition de l'oxide de polyéthylène (OPE) au bout humide de la machine peut permettre la rétention des fines particules. Cependant, le mécanisme par lequel l'OPE flocculc la matière colloidale est toujours un sujet d'actualité. Les résultats obtenus avec l'OPE et les cofacteurs (SNS, MPR et CAR) sont discutés d'après le mécanisme de pontage polymérique induit par un phénomène d'association.

La technique de la diffusion dynamique de la lumière (DLS) nous a permis d'étudier des solutions de polymère. Ces études ont révélées que les trois cofacteurs créent des complexes avec l'OPE. CAR a radicalement augmenter le diamètre apparent des chaînes d'OPE et MPR semble pour sa part le diminuer. Quand SNS est introduit dans une suspension de latex, suivant la séquence d'addition latex-polymère-cofacteur (LPC), la couche hydrodynamique (HLT) de polymère est plus épaisse. Un équilibre thermodynamique semble s'établir à une HLT d'environ 40 nm.

Des tests de flocculation a l'aide de l'analyseur photométrique de dispersion (PDA), avec l'OPE (sans cofacteur) ont suggérés que les fines n'ont pas toute les mêmes caractéristiques. Le SNS a la propriété de les rendre identiques en s'adsorbant à leur surface. Ajoutant l'OPE par la suite résulte en une homoflocculation d'où la surface spécifique des fines a pu être calculée (0.223 m^2/g).

Le mécanisme de pontage induit par association, peut se produire de trois différentes manières dépendant de l'affinité du cofacteur et de l'OPE pour les fines ou tout autre collecteur. Quand ni le cofacteur ni l'OPE n'adsorbent sur le collecteur, la flocculation peut

être initiée par les complexes OPE/cofacteur (van de Ven et Alince (1996)). Quand le cofacteur (e.g. SNS) et le polymère peuvent adsorber sur les fines, que la séquence fines-cofacteur-polymère (FCP) est utilisée et que le ratio chimique cofacteur/OPE est de 3/1, il semble que les chaînes d'OPE adsorbent sur les fines qui sont déjà couvertent par le cofacteur, suivi d'une flocculation de ces mêmes fines. Dans la séquence fines-polymère-cofacteur (FPC), si le polymère adsorbe sur les fines mais que le cofacteur adorbe ou non n'a pas d'importance, un renforcement des liens entre les particules semble survenir par l'action des molecules de cofacteurs reliant les chaînes de polymère.

ACKNOWLEDGEMENTS

I wish to express my sincere gratitude to

Prof. T.G.M. van de Ven

Prof. G. Garnier

for their encouragement, guidance and assistance, and for their dedication to this research effort. Mostly however, I wish to thank them for their trust and friendship.

Grateful acknowledgement is also made to

Dr. J. Petlicki

Dr. B. Alince

for insightful and stimulating discussions.

My warmest thanks to the people from EQUIP. International Inc. for providing the financial support.

Mr. D. Pageau

Mr. R. Brown

Mr. P. Langevin

Mr. G. Radu

Mrs. C. Hardy

and all the others for insightful discussions and contributions to this project.

My most sincere gratitude to Ondrej Drabek, Xin (Alex) Wu, Claudia Fernández, Tom Asselman, Alois Vanarek, Dr. Laipu Yu and all the other staff, graduate, and post-graduate students at the institute and department with whom I have shared one of the most memorable part of my life. I have learned much from each of them.

Many thanks also go to Dr. John Wood, Grazyna Stepien, Jocelyn Mathieu, and

Mario Grondin from Paprican for their advise and help and friendship.

Mrs. P.A. McCaffrey, Mrs. S. Shiaieb, and Mrs. McGuinness for making life as a graduate student an enjoyable experience and for all their friendship and help.

My parents, Marcel and Lise, my sister Nathalie, my brother Stéphane and all other family members for their love and support during the period of this research.

My daughter Léonie for providing me extra incentive to graduate, and finally to Guylaine, without whose love and support, this would not have been possible.

TABLE OF CONTENT

CHAPTER I

INTRODUCTION

CHAPTER II

DYNAMIC LIGHT SCATTERING OF PEO SOLUTIONS AND SUSPENSIONS OF PEO-COATED LATEX PARTICLES

CHAPTER III

STABILITY OF SUSPENSIONS OF FINES

CHAPTER IV

GENERAL CONCLUSION AND SUMMARY

APPENDIX I

PHOTON CORRELATION SPECTROSCOPY

LIST OF FIGURES

CHAPTER I

CHAPTER II

CHAPTER III

APPENDIX I

LIST OF TABLES

CHAPTER I

CHAPTER II

CHAPTER III

GUIDELINES CONCERNING THESIS PREPARATION

Candidates have the option of including, as part of the thesis, the text of a paper(s) submitted or to be submitted for publication, or the clearly-duplicated text of a published paper(s). These texts must be bound as an integral part of the thesis.

If this option is chosen, connecting texts that provide logical bridges between the different papers are mandatory. The thesis must be written in such a way that it is more than a mere collection of manuscripts; in other words, results of a series of papers must be integrated.

The thesis must still conform to all other requirements of the "Guidelines for Thesis preparation". The thesis must include: a Table of Contents, an abstract in English and French, an introduction which clearly states the rationale and objectives of the study, a comprehensive review of the literature, a final conclusion and summary, and a thorough bibliography or reference list.

Additional material must be provided where appropriate (e.g. in appendices) and in sufficient detail to allow a clear and precise judgement to be made of the importance and originality of the research reported in the thesis.

In the case of manuscripts co-authored by the candidate and others, the candidate is required to make an explicit statement in the thesis as to who contributed to such work and to what extent. Supervisors must attest to the accuracy to such statements at the doctoral oral defense. Since the task of the examiners is made more difficult in these cases, it is in the candidate's interest to make perfectly clear the responsibilities of all the authors of the co-authored papers. Under no circumstances can a co-author of any component of such a thesis serve as an examiner for that thesis.

LIST OF SYMBOLS

α	collision efficiency
β	Characteristic relaxation time
Γ	Linewith (light Scattering)
Γ_{MAX}	Maximum deposition per unit surface
ε_o	Permittivity of free space
ε_r	Dielectric constant of the medium
ϵ	(Permittivity of free space) times (Dielectric constant of the medium)
η	Number of jumps
θ	Scattering angle
Θ	Fractional coverage of a particle
κ	Debye-Hükel parameter
κ^{-1}	Debye length
λ	Constant (in van der Waals forces), and electromagnetic wavelength in the medium (in light scattering theory)
λ_0	Electromagnetic wavelength in vacuum
μ_i	Chemical potential of species i
μ	Fluid viscosity
φ	Angle change in rotary Brownian motion
χ	Energy adsorption per polymer segment
ψ	Potential function
ψ_o	Surface potential
ω	Hydrodynamic conditions parameter

a	Particle radius
a	Acceleration
A	Hamaker constant
D	Diffusion coefficient
D_r	Rotary diffusion coefficient
e	Charge of a proton
E	Energy minimum in DLVO theory
f	Translational friction coefficient
f	fraction of a given amount
f_r	Rotational friction coefficient
F	Force
F_{drag}	Drag force
F_E	Electrostatic force
F_T	Total force exerted of a particle
$\mathcal{F}_d$	Chemical force
$g^{(2)}_{BI}(\tau)$	Normalised bimodal autocorrelation
G	Shear rate
h	Distance between two colloidal particles
i_V	Intensity function from a vertically polarized incident beam
I	Light intensity
I_H	Scattered light from a horizontally polarized incident beam
I_T	Total scattered light from an unpolarized incident beam
I_U	Scattered light from an unpolarized incident beam

$\mathrm{I_V}$	Scattered light from a vertically polarized incident beam
J	Flux
kT	Thermal energy
k_{att}	Deposition rate constant
k_{det}	Detachment rate constant
k_{fast}	Fast deposition rate constant
K	Average scattering cross-section of a particle
l	Optical path length
l	Length of a single step
m	Relative refractive index ($\mathrm{m_1/m_2}$)
$\mathrm{m_1}$	Refractive index of the particles
$\mathrm{m_2}$	Refractive index of the medium
m	Mass
M	Molecular weight
$\mathrm{M_N}$	Number-averaged molecular weight
$\mathrm{M_W}$	Weight-averaged molecular weight
n	Number of possible conformations of a polymer
$\mathbf{n}$	number of particles
$\boldsymbol{n}$	Particle or ion concentration
N	Degree of polymerization
$\mathrm{P}(\theta)$	Form factor
q	Distance from the center of mass
r	Distance between a scatterer and an observer

r	Distance between two molecules
$<r^2>^{1/2}$	RMS end-to-end distance of a polymer chain
R_g	RMS radius of gyration
s_i	Radius of gyration of the ith conformation
t	Time
t_{att}	Time required to adsorb a fraction of the added polymer
t_{orth}	Time required to adsorb a fraction of the added polymer via orthokinetic collisions
t_{peri}	Time required to adsorb a fraction of the added polymer via perikinetic collisions
u	Velocity
u_o	Initial velocity
V_d	Dispersion energy interaction
V_E	Electrostatic energy interaction
V_T	Total energy interaction between two particles
w	Probability function
x	One-dimensional distance
z	Valency of electrolyte

CHAPTER I

INTRODUCTION

1.0 INTRODUCTION

The Paper Industry is in constant evolution, seeking for higher paper machine speed, efficiency and paper quality (like opacity). These three factors can be attained by increasing the first-pass retention. A lower consistency of the white water is the result of higher retention, allowing faster drainage and consequently, a higher speed of the paper machine. The efficiency of a paper machine is defined as the ratio of the total production, over the theoretical production if no break of the sheet and no reject occurred. The paper quality improvement, which is revealed by the higher efficiency, can often be achieved by retaining the small particles in the forming sheet. Small particles can be either fines (very small wood fibers) or fillers like calcium carbonate, clay or titanium dioxide. One of their roles is to fill the cavities (or voids) between the big fibers, increasing the opacity of the sheet.

The problem is that, due to external forces, the finer particles are hardly captured by the sheet of paper during its formation. Hydrodynamic forces are very important at the wet-end of a paper machine. The consistency of the pulp suspension passes from about 1% to 20%. This means that approximately 95 tons of water must be removed within a few seconds for each ton of paper produced [1]. This is achieved by filtering the pulp suspension on a synthetic polymer fabric. Two mechanisms are operating in retention: filtration and adsorption. Filtration is more important for fibers, big fines and aggregates while adsorption occurs for smaller particles like small fines and fillers (colloidal particles). Typically, pulp fibers have a length of a few millimeter, while the fines and colloidal substances range from a fraction of one μm up to 150 μm.

Adding retention aids like neutral polymers or polyelectrolytes (charged polymers), at the wet end of a paper machine can result in an increase of the filler retention from near zero to 50 or 60 percent [1]. This can only be achieved only if the physicochemical conditions are significantly changed [2]. Among the polymers of commercial interests, polyethylene oxide (PEO) is widely used for newsprint and groundwood specialties. PEO has gained wide acceptance in the industry for its performance and low cost. In addition of retaining the fines and fillers, it is retaining the wood resins in the forming sheet, decreasing the frequency of problems related to pitch deposition.

However, controversy is still surrounding the mechanism by which PEO retains the colloidal particles [3]. The bridging mechanism was first proposed. PEO was found less sensitive to the anionic contaminants found in a pulp suspension than the usual cationic polyelectrolytes, and was thought to bridge fillers and fibers together. Experiments proved that PEO often works in systems where it does neither adsorb on fibers nor on fillers. Pelton and al. [4] found that PEO often needs a second component to be efficient and it was suggested that dissolved lignin contributes to a synergistic adsorption. This second component is referred to as a cofactor or enhancer. Later, Lindström and Glad-Nordmark [5] proposed the network mechanism where there is no adsorption on fibers nor on fillers. Rather, a three-dimension network is formed in which the filler particles are captured and then swept up by the big fibers. Van de Ven and Alince [3] argued against this network mechanism for weak hydrodynamic and thermodynamic foundations, and instead proposed the mechanism of association-induced polymer bridging. The principle is that a freely dissolved PEO molecule is more easily adsorbed onto a collector when its configuration has been modified by a cofactor. The proposed mechanism can happen either if a cofactor adsorbs or not onto the collector (fibers). Depending on the type of cofactor used, the PEO/cofactor complex has been found to vary the flocculation efficiency.

The **objective** of the present study is to investigate the mechanisms by which the PEO/cofactor association can retain the fines during the paper formation process and to explain these differences in efficiency. Three different classes of cofactors were selected: carbamide (CAR), sodium naphthalene sulphonate (SNS), and modified phenolic resin (MPR). The **hypothesis** investigated is that a pulp suspension is flocculated by PEO/cofactor association via the association-induced polymer bridging mechanism [3]. A series of PEO/cofactor properties should be elucidated to characterize a particular cofactor.

The strategy (Figure 1) selected combines two techniques: the dynamic light scattering (DLS) and photometric dispersion analysis (PDA). The former technique was used to follow the change in PEO chain configuration as a cofactor is added to a polymer solution. Other experiments on adsorption of PEO onto latex particles gave a hydrodynamic layer thickness as a function the cofactor type, cofactor/PEO ratio, and time. Latex suspensions were chosen for their well known surface properties and spherical shape. Moreover their surface charge is similar to that of wood fibers. The second technique (PDA) can best measure the stability of wood fines suspensions in the presence of PEO/cofactor associations. This system was closer to and industrial application by using a wood suspension with comparable shear rate and electrolyte concentration. The stability was measured as a function of PEO concentration, the sequence of addition (cofactor prior to PEO or the inverse,) and the cofactor/PEO ratio. A better understanding of the mechanisms can lead to significant improvement of fines and fillers retention during papermaking.

This Introduction chapter (chapter I) presents the basic theory and summarizes the literature overview that is necessary to understand the more specific

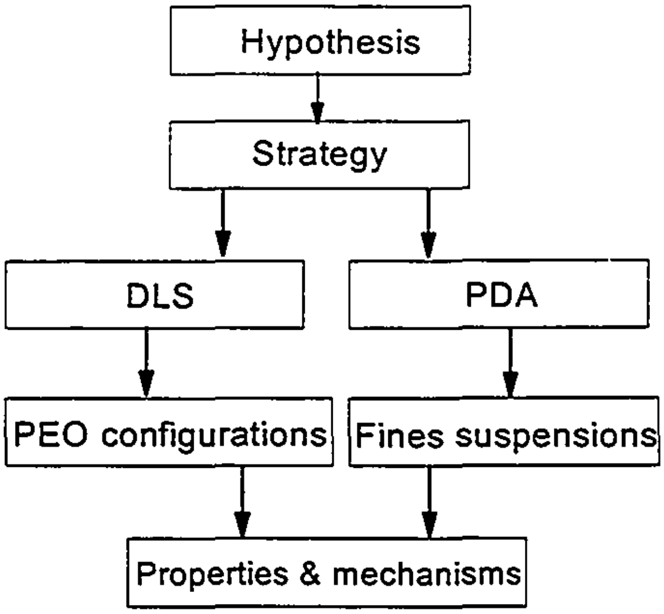

Figure 1: Strategy plan of experimental work.

subjects of the two subsequent experimental chapters. The work begins in describing the Brownian motion to calculate the diffusion coefficient of a colloidal particle. The Brownian motion is one of the external forces that bring particles together to destabilize a colloidal suspension. The stability of colloidal suspensions is the subject of the following section, where it is question of particles interactions, and polymer chemistry and physics. A literature review is also presented at the forth section. It is question of PEO behavior in solution, and in suspensions of latex particles or wood pulp fibers. The emphasis is put on the interaction of PEO and cofactor and the lastly proposed flocculation mechanisms. Finally, the last part is concerned with the light scattering theory to introduce light as the probe for the experimentation of that research project.

2.0 BROWNIAN MOTION

2.1 General concept

Optical microscopic observations of small particles dispersed in water reveal a constant state of random motion. The discovery of the phenomenon is attributed to Robert Brown (1828). He observed the perpetual motion of plant pollens under a microscope and thought that these particles were "alive." Controversy persisted until Gouy (1888) ruled out extraneous causes and focused attention on molecular agitation. In 1910 Perrin concluded that the particles seem to move independently with no effect of density or composition, although the amplitude of the motion is greater for smaller particles, with less viscous fluid and higher temperatures. According to van de Ven [6], the Brownian motion can be described as the perpetual motion executed by small suspended particles due to fluctuations in the force exerted on them by the molecules of the suspended fluid. Under normal conditions a Brownian particle will suffer about 10^{21} collisions per second with fluid molecules, leading to the chaotic motion of the particle.

The Brownian motion can be quantified by finding the diffusion coefficient, *D*, of the suspended particles. This is the result of the development shown below. The Brownian motion is first characterized in terms of the length of one single step and the time taken by a particle to travel such a distance. The random walk analogy is derived to obtain the root mean square (R.M.S.) distance traveled by a particle as a function of time. The last of the Brownian motion sections is the application of the diffusion laws to obtain the diffusion coefficient, *D*.

There are two kinds of Brownian motion: translational and rotational. Spherical particles show translational motion (Figure 2) and non-spherical particles illustrate

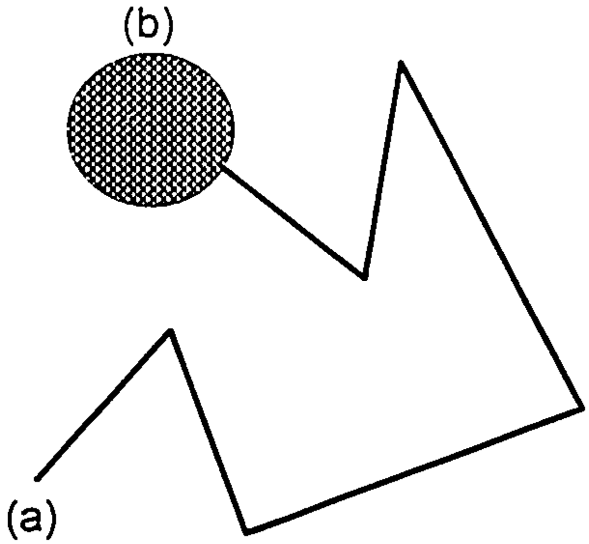

Figure 2: Translational Brownian motion from point a to point b, of a non-interacting particle.

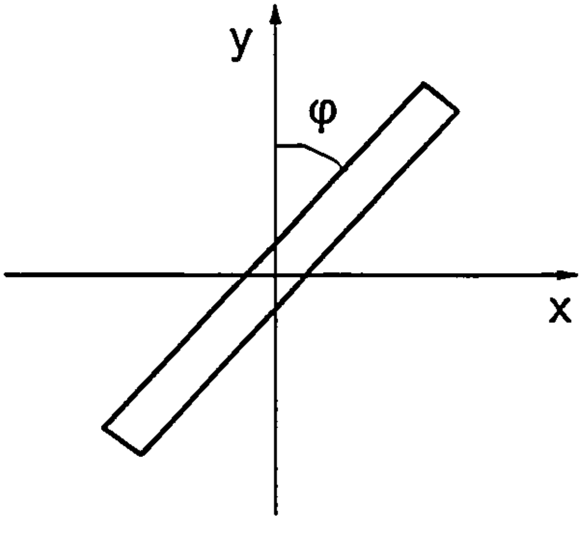

Figure 3: Rotational Brownian motion leading to a change in orientation of a rod shaped particle.

translational and rotational motion (Figure 3).

The length of a single step in translation or the angle change in rotation, depends on the rapidity of the observer. It can be explained by measuring the contour of an island on maps of different scales. The details of the contour are more visible on a 1:20000 scale map than on a 1:100000 scale. In the same way of thinking, if the stochastic motion of a particle is filmed, the apparent distance a particle travels depends on the time frame used in observing the particle [6]. This is called a self-similar phenomenon.

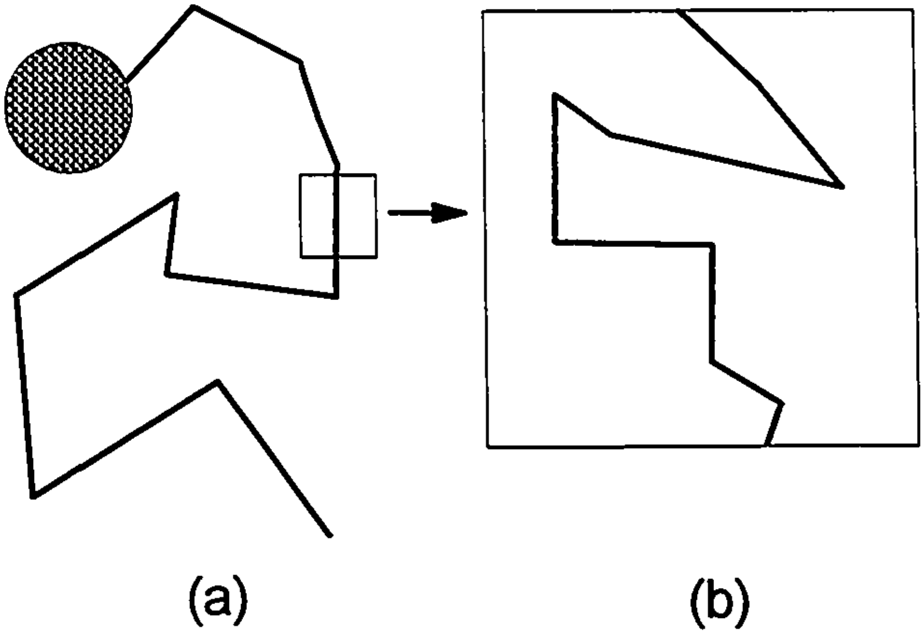

Figure 4: Self-similar phenomenon of Brownian motion. Enlargement of a portion of (a) is presented in (b). Qualitatively similar form of the trajectories is shown.

Therefore, the velocity of a particle at a given position is meaningless. More useful is the relation of the approximated displacement and orientation. Stokes law describes the drag force, F_{drag}, experienced by a particle moving in a fluid.

$$F_{drag} = -fu \tag{1}$$

The variable u is the particle velocity. The friction coefficient $f = 6\pi\mu a$ being the Stokes-Einstein equation in which μ is the fluid viscosity and a is the particle radius. Combining the drag force with Newton's second law,

$$F = ma \tag{2}$$

where m is the mass and a, the acceleration, we get,

$$ma = -fu \tag{3}$$

Equation 3 can be rewritten for a one-dimensional displacement as,

$$\frac{d^2x}{dt^2} = -\beta\ \frac{dx}{dt} \tag{4}$$

where $\beta = f/m$. The solution to this differential equation is,

$$x = \frac{u_o}{\beta}\left(1 - e^{-\beta t}\right) \tag{5}$$

where u_o is the initial velocity, and β is regarded as a characteristic relaxation time, or the time taken by the particle for a single jump of the particle. The length, l, of a single step can be calculated from equation (5) for $t \to \infty$,

$$l = x(t=\infty) = \frac{u_o}{\beta} \tag{6}$$

where u_o is evaluated from the equipartition of energy for a particle in thermal equilibrium with the medium [6]. The final result is,

$$l \approx \frac{(mkT)^{1/2}}{f} \tag{7}$$

in which kT is the thermal energy. For example, a particle of one micrometer in water at 25 °C, has a calculated characteristic relaxation time, β^{-1}, of 2.5x 10^{-7} s, and a single step length, l, of 0.25 nm (after van de Ven [6]).

2.2 Random walk

The Brownian motion can be defined as a series of jumps of irregular magnitudes and in arbitrary directions. To describe the displacement of a particle in space, we can consider a one-dimensional system (frame of reference). Lets assume that each jump is of the same size and has an equal probability of being in the forward direction. The probability, *w*, of finding the particle at a position, x, at a time, t, is:

$$w(x,t) = \frac{1}{(2\pi\eta l^2 t)^{1/2}}\, e^{-\left(\frac{x}{2\eta l^2 t}\right)} \tag{8}$$

which is the normal distribution function, where η represents the number of steps. This well-known bell curve is flattening with time because the particle is quitting its initial position.

Even if the average displacement is zero, the important result is the mean-square displacement, $<x^2>$:

$$<x^2> = \int_{-\infty}^{+\infty} x^2 w(x,t)\,dx \; = \; \eta l^2 t \tag{9}$$

The random walk is a good approximation of the Brownian motion. However the solution is not exact and without going into details, the correct result is derived from the equation of Langevin [6, 7].

$$<x^2> = \frac{2kT}{f}\, t \tag{10}$$

Equivalently, for the rotational Brownian motion, $<\Delta\varphi^2>$, of a rod shaped particle,

$$<\Delta\varphi^2> = \frac{2kT}{f_r}\, t \tag{11}$$

in which f_r is the rotary friction coefficient. The generalization of the random walk for an ensemble of particles is described by the Brownian diffusion in the next section.

2.3 Diffusion

The diffusion of colloidal particles can be either explained by a driving force resulting from a gradient in the chemical potential through the suspension, or by the stochastic movements of each particle. Imagine a box initially separated in two parts like the one of Figure 5.

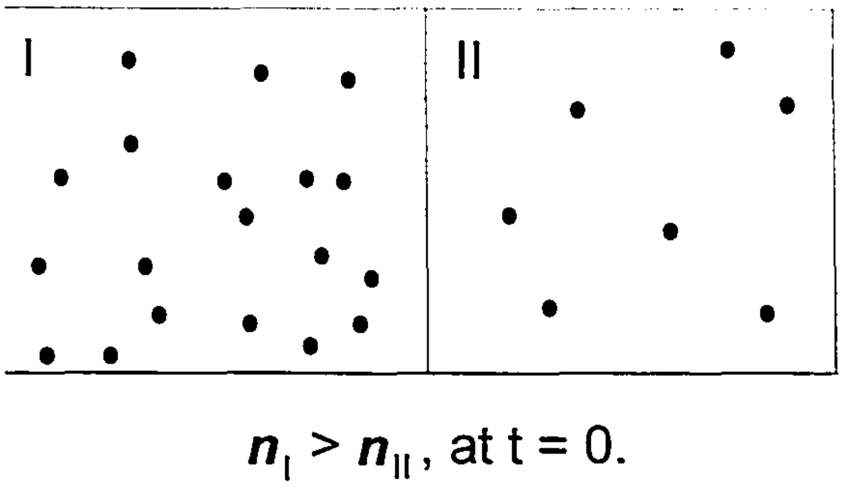

Figure 5: Box initially separated in half. At time equal to zero, concentrations of both sides I and II are to equilibrate by Brownian diffusion.

Initially, the concentration n_I is greater than n_{II}. The one-dimensional chemically driven force, $\mathcal{F}_d$, is,

$$\mathcal{F}_d = -\frac{d\mu_i}{dx} \tag{12}$$

where μ_i is the chemical potential. As long as a chemical potential gradient exist through the volume, a driving force will equalize the particle concentration by diffusion. Statistical analysis leads to the same result: each particle is likely to move to the left or to the right due to its chaotic Brownian motion. Since there are more particles in the container I than in II, there will be a net movement of particles towards the latter side.

The flux of material, J, is proportional to the concentration gradient given by Fick's first law of diffusion,

$$J = -D\frac{dn}{dx} \tag{13}$$

in which, D, is the coefficient of diffusion of a particle. The definition of the diffusion coefficient is:

$$D = \frac{kT}{f} \tag{14}$$

It is one of the many important equations attributed to Einstein [6, 8-11]. The diffusion coefficients for translation and rotary Brownian motion are given in Table I for spherical particles. Diffusion coefficients can also be derived for non-spherical particles and aggregates [6, 9].

The first Fick's law of diffusion describes steady-state only. In a transient process, without convection, and where D is a constant, the Fick's second law of diffusion is,

$$\frac{\partial n}{\partial t} = D\nabla^2 n \tag{15}$$

The solution of this equation for a point source at the origin (in x-direction) is,

$$u(x,t) = \frac{1}{2(\pi D t)^{1/2}} e^{-x^2/4Dt} \tag{16}$$

Comparing equation (16) with equation (8), the random walk can be regarded as a diffusion process with $D = \frac{1}{2} nl^2$. Equation 9 then becomes,

$$\langle x^2 \rangle = \int_{-\infty}^{+\infty} x^2 \eta(x,t)\,dx = 2Dt \qquad (17)$$

Similarly derived for rotary Brownian motion.

$$\langle \varphi^2 \rangle = 2D_r t \qquad (18)$$

The theoretical diffusion coefficients can then be calculated for a given particle size.

Table I: Calculated values of diffusion coefficients (translation and rotation), for various sized spheres in water at 25°C (after van de Ven [6]).

a (μm)	D (m^2s^{-1})	D_r (s^{-1})
0.001	2.2×10^{-10}	1.7×10^{8}
0.01	2.2×10^{-11}	1.7×10^{5}
0.1	2.2×10^{-12}	1.7×10^{2}
1	2.2×10^{-13}	1.7×10^{-1}
10	2.2×10^{-14}	1.7×10^{-4}

These values are for non-interacting particles at low concentration. The particles experience collisions during Brownian motion. These collisions may lead to coagulation or flocculation, it is then worthwhile to develop on the topic of the stability of colloidal suspensions.

3.0 STABILITY OF COLLOIDAL SUSPENSIONS

The ability to apply colloidal science to technical problems fascinated Faraday 140 years ago [10], and is still a challenge nowadays. Typical colloidal systems are heterogeneous, thermodynamically and aggregately unstable owing an interface between particles and the dispersion medium [12]. Fennel Evans [10] gives an example of a stable colloid suspension that we see every day, the milk. Milk is a suspension of proteins (casein) and fat globules. This suspension is remarkably stable up until the pH is changed. Adding acid like lemon juice, or letting the milk at ambient temperature for too long will give the same result. In the latter case, microbial activity results in the production of lactic acid and will also change the pH of the suspension. This change in pH neutralizes the charges of the proteins and induces coagulation. There, you know how to make yoghourt!

In the absence of polymers and polyelectrolytes, there are traditionally two types of interactions operative in a colloidal system: the van der Waals and the electrostatic (double-layer) interactions. These forces are presented in the next sections followed by the DLVO theory (Derjaguin, Landau, Verway, and Overbeek). Other forces like hydrodynamic conditions are also important and whether deposition takes place or not depends on the net interaction energy between the particles and the collector [13]. A brief description of the effect of adding polymers to a suspension is also given.

3.1 Van der Waals dispersion forces

The van der Waals forces are attractive for identical substances and can be either attractive or repulsive for different substances. Arising from electromagnetic interactions, they are of three types: London, Keesom and Debye. The first type, London, describes interactions between two neutral molecules; the second type, Keesom, represents the interactions between molecules with permanent dipoles; and thirdly, Debye interactions occur between polar and neutral molecules. All three types are called dispersion forces and their combination, written in terms of the dissipation energy, V_d, is:

$$V_d = -\frac{\lambda}{r^6} \tag{19}$$

in which, λ, is a constant depending on the nature of the material and r is the distance between two molecules. For two colloidal particles consisting of a large quantity of molecules, the dispersion energy is obtained by adding the contribution of each one. For two identical spheres interacting with each other [6], the dissipation energy is:

$$V_d = -\frac{A}{6}\left(\frac{2a^2}{(h^2+4ah)} + \frac{2a^2}{(h+2a)^2} + \ln\frac{(h^2+4ah)}{(h+2a)^2}\right) \tag{20}$$

In which, A, is the Hamaker constant, and h, is the distance separating them. This result is a good approximation but is not exact because of the retardation effects, and the influence of the neighboring molecules were neglected. However the present development is sufficient for the present study but the interested reader is referred to the theory of Lifshitz and co-workers [6, 10].

3.2 Electrostatic double-layer interactions

In most cases, colloidal particles possess electrostatic charges, creating a double-layer. The electrostatic force of interaction between two particles is derived below. The principle of electroneutrality establishes that the net charge in the dispersion medium is equal, but opposite in sign to that of the particles. The counterions in the dispersion medium give rise to the electrical double layer that surround the colloidal particles [14]. One of the most important equation of statistical physics, is the Poisson-Boltzman equation, since it is the basis of our understanding of electrolyte solution, electrode processes, colloid interaction, membrane transport, nerve conduction, transistor behaviors, and even plasma physics [8].

$$\nabla^2\psi = -\frac{1}{\varepsilon_o\varepsilon_r}\sum n_i^o z_i e \ \exp\left(\frac{-z_i e\psi}{kT}\right) \qquad (21)$$

in which ψ is the potential; ε_o and ε_r are the permittivity of free space and the dielectric constant of the medium respectively; n_i^o is the bulk concentration of ions of type i; z_i is the valency of the salt; and e, is the charge of a proton. The equation (21) gives the profile of the potential as a function of the ion concentration. The Poisson-Boltzman equation is accurate in its representation of the diffuse double-layer potential [8]. From the Debye-Hückel approximation of the above equation, came an important parameter called the Debye-Hückel parameter, κ,

$$\kappa = \left(\frac{e^2\sum n_i^o z_i^2}{\epsilon kT}\right)^{1/2} \qquad (22)$$

in which $\epsilon=\varepsilon_o\varepsilon_r$. The extent of the double layer surrounding a colloid is measured by the parameter κ^{-1}, the region of variable potential. Also called the Debye length, κ^{-1} can be varied by changing the concentration and the valency of an electrolyte. Typically, κ^{-1} varies from about 100 nm at 10^{-5} M to less than 1 nm at 10^{-1} M [6, 14].

When two particles are brought together, their double-layers overlap. The resulting effect is that the ions and potential distribution are no longer symmetrical around the particles. Surface forces become relatively important at that time. Derjaguin (1934) made a useful approximation to replace particles with curved boundaries by a series of infinitesimally thin cylinders [6]. The result is valid for relatively large particles with constant surface charge. This is known as the Derjaguin approximation.

$$F_E = \frac{B\pi a}{\kappa}\exp(-\kappa h) \tag{23}$$

$$B = \frac{32\gamma_o^2\epsilon\kappa^2(kT)^2}{(ze)^2} \tag{24}$$

$$\gamma_o = \tanh\left(\frac{ze\psi_o}{kT}\right) \tag{25}$$

In which F_E is the force (repulsive for identically charged particles) exerted by the electrical double-layer, and ψ_o is the surface potential.

The knowledge of both of the dispersion and electrostatic interactions, equations (20) and (23) respectively, leads to the DLVO theory presented thereafter.

3.3 Total potential energy interaction and classical DLVO theory

The stability of colloidal suspensions can be described by the sum of the interaction energies. Derjaguin and Landau (1941) and Verway and Overbeek (1948) (DLVO), combined the van der Waals dispersion forces with the electrostatic double-layer forces to explain the stability of lyophobic colloids. The free energy of interaction between the particles is related to the force by,

$$F_T = -\frac{\partial V_T}{\partial r} = -\left(\frac{\partial V_d}{\partial r} + \frac{\partial V_E}{\partial r}\right) \tag{26}$$

Interaction potentials have the character of free energies and contain energetic and entropic contributions. For the case of two identical spherical particles the total free energy is approximated by,

$$V_T = -\frac{Aa}{12h} + c\ \exp(-\kappa h) \tag{27}$$

where c is an integration constant.

The van der Waals attractions dominate at small and large distances. Very close to the wall, V_E approaches a finite magnitude, whereas V_d goes to some very low values, attracting particles into deep intimate contact. This well, called primary minimum, is not infinitely deep. Very short range energy repulsion arises between the atoms on each surface. This is called the Born repulsion. Hunter [8] introduced the so-called solvent-structural term, V_S, in which the Born repulsion is included. Observation of stable colloidal suspensions even at very high electrolyte concentration have lead to this extra term in the total energy interaction equation.

$$V_T = V_d + V_E + V_S \tag{28}$$

The secondary minimum, which occurs at larger distances (~7 κ^{-1}), is also important in colloidal suspensions. Coagulation into the primary minimum is sometimes irreversible or very difficult to redisperse. Flocculation occurs when particles are entrapped into the secondary minimum. Application of mechanical energy can easily break the later flocs. The height of the energy barrier in Figure 6, determines the stability of the suspension. A typical value of the energy barrier for a stable suspension is greater than about 10 kT. The height of the barrier can be varied by ionic strength or surface potential. For example, At high ionic strength and where DLVO applies, the energy barrier disappears and fast coagulation occurs.

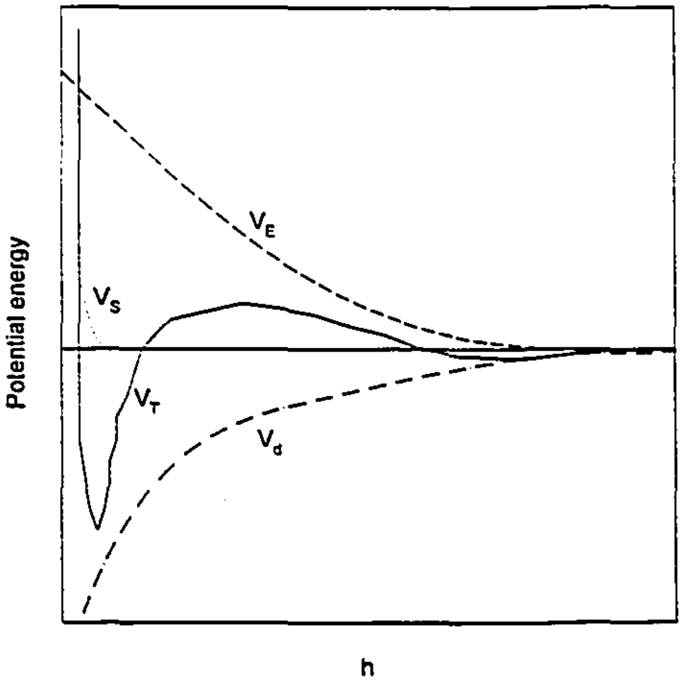

Figure 6: Total potential energy of interaction $V_T=V_d+V_E+V_S$ where V_s is the potential energy due to solvent layers (after Hunter [8]).

The addition of macromolecules like polymers can completely transform the behavior of a colloidal suspension by changing the nature of the interactions between the particles. The next section is concerned with that phenomenon.

3.4 Addition of polymers in colloidal suspensions

Polymers are used to stabilize or destabilize a colloidal suspension when one cannot change the electrolyte concentration or the surface properties of the particles. General features about neutral polymer behavior in solution are given in the next section, comprising the radius of gyration, and whether or not the polymer chains adsorb onto a surface.

The two most widely used molecular weight averages are the number-average, M_N, and weight-average, M_W [15].

$$M_N = \frac{\sum_i n_i M_i}{\sum_i n_i} \tag{29}$$

$$M_W = \frac{\sum_i n_i M_i^2}{\sum_i n_i M_i} \tag{30}$$

In which, n_i, is the number of molecules having the molecular weight, M_i. M_N/M_0 is the number-average degree of polymerization, where M_0 is the molecular weight of the monomer. The M_W is always greater than M_N because longer polymers contribute more to the weight than to the number average value. Other averages are also used and the reader is referred to [15] for more details. The polydispersity (or the ratio of weight average over number average) is an indicator of the width of the size distribution. It is usually varying from one to three and a value of two is obtained for a purely random termination reaction [10].

The conformation of polymer molecules is critical in the stability of colloidal suspensions. The number of conformations accessible to a normal carbon backbone polymer in a very dilute solution is of order 2^b, where b is the number of bonds in the polymer. Some biopolymers have a relatively fixed conformation like a rigid rod of a length, L, scaling as the degree of polymerization, N. On the other hand, compact globules have a radius, $a \sim N^{0.3}$ [10]. Synthetic polymers tend to adopt a more flexible conformation, where the radius of gyration $R_g \sim N^{\alpha}$, and $0.5 < \alpha < 1$ [10]. The value of α depend on conformal restrictions like valency angles. One parameter to specify the size of a linear polymer molecule is the root-mean-square end-to-end distance, $<r^2>^{1/2}$. This quantity is sometimes ambiguous, especially for branched polymers [14]. One more commonly used measure of the polymer size is the RMS radius of gyration, R_g:

$$R_g = <s^2>^{1/2} = \left(\frac{\sum n_i s_i^2}{\sum n_i} \right)^{1/2} \tag{31}$$

$$s_i = \left(\frac{\sum m_{ij}\; q_{ij}^2}{\sum m_{ij}} \right)^{1/2} \tag{32}$$

where, n_i, is the number of conformations, s_i is the radius of gyration of the ith conformation, m_{ij} is the mass of the jth element in the ith conformation, and q_{ij} is the distance of the jth element from the center of mass in the ith conformation. R_g corresponds to an averaged radius of polymer chains [14, 16], and can be measured by light scattering, or viscosity.

Attached polymer chains on surfaces

Free polymers in solution can either adsorb onto a surface or stay in solution, depending on several parameters like the quality of the solvent and the affinity of the polymer for the surface. Homopolymers adopt special conformations when adsorbed on surfaces. Figure 7 illustrates a homopolymer adsorbed on a colloidal particle with tails, loops and trains. A polymer can adsorb on the surface of a colloidal particle via four types of interactions: Coulombic (charge-charge), dipole interactions, hydrogen bounding, or van der Waals dispersion forces.

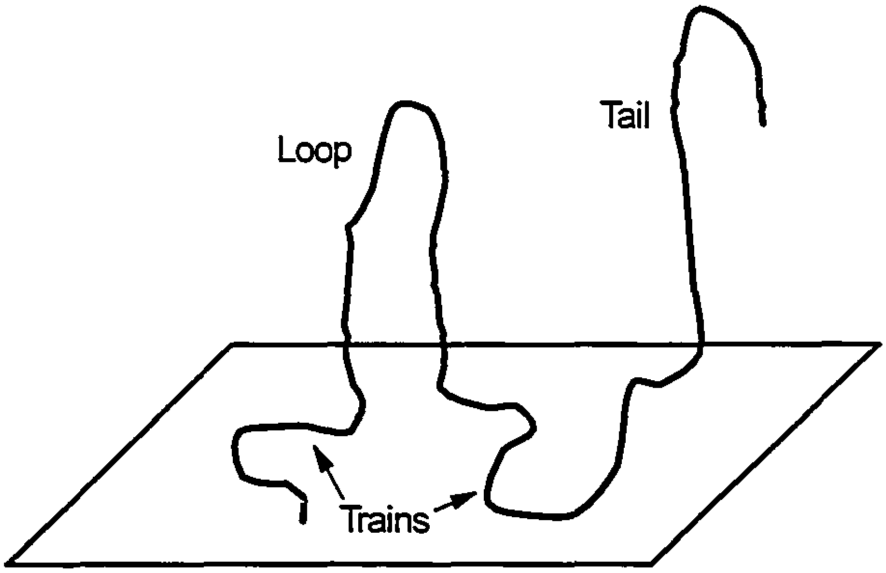

Figure 7: Schematic diagram of a polymer adsorbed on a surface (after Hunter [8]).

The early makers of inks and paints were well aware of the value of certain natural gums in promoting the stability [8]. The surface of the lyophobic colloidal particle was covered with a lyophilic polymer from which tails and loops were extending into the solution. In that case, the interactions between lyophilic polymer chains impart stability. Depending on the amount of a neutral polymer added to a colloidal suspension, flocculation or steric stabilization may occur. Steric stabilization is of great importance in colloid science. Two conditions are required for stearic stabilization: full coverage of the particles surface by the polymer and an adsorbed polymer layer thickness extending over the electrical double-layer range. For example, Table II illustrates the importance of the polymer extent (RMS end-to-end distance) into solvent compared with the double layer thickness (κ^{-1}). The spatial extension a of neutral polymer is function of its molecular weight, and the double layer thickness is a function of the electrolyte concentration.

Table II: Theoretical calculations of the spatial extent of polymers of different molecular weight and, the extent of the electrical double layer at different salt concentrations (after Hunter [8]).

1:1 electrolyte concentration (mol/l)	Double-layer thickness (nm), κ^{-1}	Polymer molecular weight	Spatial extension (nm)
10^{-5}	100	10^{6}	60
10^{-4}	30	10^{5}	20
10^{-3}	10	10^{4}	6
10^{-2}	3	10^{3}	2
10^{-1}	1		

These numbers clearly show that polymers of a relatively low molecular weight will extend in space over distances where van der Waals attractions are effective.

Flory-Huggins (1941) came with a theory based on free energy of mixing to explain the interactions between adsorbed polymers on approaching colloidal particles. Extensive work has been done by Napper (1983) in stearic stabilization.

If the first condition for steric stability fails by means of insufficient polymer chains to cover the colloids surface, but the second condition regarding the spatial extension is met, flocculation may occur when two colloidal particles collide. During such a collision, the adsorbed polymer molecule on one particle can adsorb on the bare surface of the other, creating a bridge between them. Ruehrwein and Ward (1952) were the first to propose this bridging mechanism. The theory predicts that the maximum flocculation efficiency is reached at half coverage of the suspended particles by the polymer [17]. How fast this flocculation occurs is the subject of the following lines.

De Gennes [18] has greatly contributed to the understanding of the thermodynamic equilibrium of adsorbed polymers on a single surface or bridging two surfaces. However, most of the adsorption processes are kinetically controlled over a very long period of time, like days, months or even longer (after van de Ven [19]). The deposition and detachment kinetics of polymers and fillers can rather be modelled by a modified Langmuir equation [2, 19, 20],

$$\frac{d\Theta}{dt} = k_{att}(\varsigma_0 - \Theta)(1 - \Theta) - k_{det}\Theta \tag{33}$$

where, Θ, is the fractional coverage of pulp fibers by the colloids or the polymer chains; k_{att} is the deposition rate constant; k_{det} is the detachment rate constant; and ς_o is the initial concentration of polymer, c_o, divided by the maximum amount that can deposit in a unit volume of the suspension, containing 1 g of pulp fibers.

$$\varsigma_0 = \frac{c_0}{\Gamma_{MAX}} \tag{34}$$

Here c_0 is the initial polymer concentration expressed in grams of polymer per gram of pulp fiber. Γ_{MAX} is the maximum amount that can deposit in the same units (g/g). The deposition rate constant is defined as,

$$k_{att} = \alpha k_{fast} \tag{35}$$

Where, α, is the deposition efficiency between two particles, and varies from 0 to 1. k_{fast} is dependant on hydrodynamic forces. The detachment rate constant is,

$$k_{det} = \omega e^{\frac{-|E|}{kT}} \tag{36}$$

This detachment rate depends on two factors, the hydrodynamic conditions ω and the depth of the energy minimum E (from DLVO theory). E depends on the chemical nature of the bonding between two particles. A retention aid is added to a papermaking suspension to change and obtain the desired values of α^{cf}, α^{cc}, E^{cf} and E^{cc}, where "c" refers to colloids and "f" refers to fibers. Kinetics of polymer bridging of particles are always coupled to slower kinetics of polymer adsorption.

Free polymers in solution

Free polymers, which are often present in biological dispersions or in a drying paint film for example, can also induce flocculation without adsorbing to any surface. This phenomenon is called Depletion Flocculation, and happens when two colloid particles approach so closely that polymer chains are excluded from the inter-particle region. The pure solvent being in the gap will have a tendency to escape, equalizing the chemical potential with the bulk solution, and creating an osmotic pressure favorable to flocculation process.

4.0 LITERATURE REVIEW ON THE POLYETHYLENE OXIDE

The fact that polyethylene oxide (PEO) is the simplest structure of water soluble polymer and its wide range of applications, has made it one of the most extensively studied.

General properties of the polymer and its interactions with other chemicals or colloids are reviewed. The PEO was first used as a single component in retention aid systems, and thereafter other chemical compounds were added for their synergistic effects in combination with PEO. In this section, flocculation mechanisms are discussed from the classical bridging to the association-induced polymer bridging.

4.1 Polyethylene oxide characteristics

The synthesis of high molecular weight PEO is made by heterogeneously catalysed polymerization of ethylene oxide [21]. However, the molecular weight distribution is very wide ($M_W/M_N \approx 20$) and narrow-range samples require fractionation. The problem is that the bulk polymer is highly crystalline at ambient temperature ($T_M \approx 66\,°C$) so that sophisticated separation methods should be used. The glass transition, $T_G \approx -55\,°C$. The density at 25°C, can vary from 1.13 to 1.23 g/cm^3 for amorphous and crystalline states respectively. The PEO is a nonionic polymer: the molecules do not carry charges. It is also a homopolymer: a molecule of PEO consists of only one monomer unit repeated N times. The following chemical formula represents a PEO molecule:

$$-\left(-CH_2-CH_2-O-\right)_N- \qquad (37)$$

The molecular weight of the monomer is 44.05 and the degree of polymerization can be greater than six million.

The absence of double-bonds (except for chain terminations) and its linear (not branched) constitution allow the PEO chain to be very flexible and to form a random coil conformation. The ether oxygens are though to create hydrogen bonding with other substances [22-25], enhancing the PEO solubility, and its ability to create association-complexes. The ethylene group (—CH_2—CH_2—) is hydrophobic [26, 27] and contributes to the adsorption of the molecules onto hydrophobic surfaces. PEO does not adsorb onto pure cellulose [28, 29], but does adsorb onto the residual lignin sites on fibers or fines [30]. Lignin residues are hydrophobic. The polyether oxygens of PEO and acidic protons of phenol groups of substances present in pulp suspensions, are responsible for hydrogen bonding. Then, a PEO chain can adsorb onto residual lignin patches by both of its hydrophobicity and its ability to share electrons from the ether oxygen. Thermal analysis experiments (differential scanning calorimetry) brought the evidence of hydrogen bonding between PEO and a cellulose model (2,3-di-O-methylcellulose) [31], but this interaction is not strong enough to be notified in flocculation processes. Degradation of the PEO chains in solution has been reported in presence of oxygen and light [21]. The PEO seems to undergo autoxidation reactions (characteristic of ethers) and is catalyzed by traces of metal ions. This may be prevented by adding antioxidants such as hindered phenols. The presence of these anticxidants may affect the conformational size of the polymer in solution. Another study concluded that the primary reason for long term instability is related to the presence of small quantities of hydroperoxides or related substances in the initial polymer [21, 32]. It was also found that chains scission occurred at high shear [33]. In most of these studies, the degradation is evidenced by a loss in solution viscosity in time.

High molecular weight PEO is hardly dissolved in water. It is believed that a fresh, clear solution contains entangled PEO molecules, clusters and free coils. At equilibrium, above a critical self-association concentration, only the clusters and free coils coexist in a thermodynamic equilibrium [34]. The disappearance of the entangled molecules may contribute to the loss in viscosity. The clusters contain a few hundred polymer chains, and the diameter was found to be about 400 nm, independently of the molecular weight. Such a PEO solution is to be added to a pulp suspension.

Wood fibers have been extensively studied and found to have a porous rough surface [35]. The polymer molecules can penetrate into the fibers through these pores [36, 37]. Furthermore, pulp fibers and fines are very different in terms of surface properties, size, and shape. A rather simpler model, such as latex particles, is therefore ideal to characterize the adsorption and configuration of PEO chains. The adsorption steps, the equilibrium hydrodynamic layer thickness of adsorbed polymers [38, 39], the stability of latex suspensions in presence of neutral polymer [17, 40], as well as the latex characteristics [41], are variables of direct interest in papermaking.

When a polymer solution is added to a wood pulp suspension, many situations may happen depending on which surface is coated with polymer [42]. Considering that fibres are the solid surface and the fines or fillers are the particles, the possibilities are: (i) polymer-coated particles and a bare solid surface, (ii), the particles and the solid surface coated with polymer, and (iii), bare particles and a polymer-coated surface. The polymer can also be in excess or not, resulting in 6 possibilities. A seventh possibility arise from the distinct character of PEO. It is known to flocculate pulp suspension even if it adsorbs neither on the particles nor onto the solid surface (see section 4.3).

4.2 Polyethylene oxide in papermaking

The use of PEO as a retention aid for papermaking started in the 1950s [43]. The application became important in the 1970s and the classical bridging mechanism was though to be the explanation for the PEO effectiveness [4, 28, 29, 44]. Later, it was found that flocculation of pulp suspension by PEO was significantly enhanced by adding a second chemical referred to as a cofactor or enhancer. In 1978, Carrard and Pummer [45] were awarded a patent on the use of PEO and phenol-formaldehyde resin. Later results on kraft lignin, being inexpensive and improving significantly the retention with PEO, lead to an other patent issued in 1982 by Pelton et al. [46]. Several other patents on the combination of PEO and cofactors were also issued but are less widely used.

Makedown procedures of PEO stock solutions are crucial in retention efficiency [47]. It was concluded that running at low makedown PEO concentration and minimizing the use of filters on the feeding line, prevent important viscosity drop. This might be related to the presence of entangled molecules in a fresly dissolved PEO solutions (section 4.1). Minimizing the shear in the filters by lowering the PEO concentration may decrease the entanglements break up.

One requirement for the effectiveness of PEO in flocculating pulp suspensions is that the molecular weight should be greater than $4 \cdot 10^6$ [4, 28, 44, 48]. When adsorbed onto a particle, shorter chains may not extent far enough into the bulk solution to overcome the electrostatic interactions.

Prior to the 1980's, PEO was most often used as a single component. Conventional polyelectrolytes were found ineffective in pulp suspensions characterized by very high amounts of dissolved and colloidal materials. Conversely, the retention aid system with PEO was more effective in that case [4, 22, 48-50]. Indeed, the materials detrimental for polyelectrolytes were enhancing the efficiency of PEO. The retention efficiency was varying considerably depending on the species of the beneficial contaminants.

Then the addition of a cofactor started. PEO was already known for long time to form complexes with small molecules structures [21]. Analysis of pulp suspensions contaminants also contributed to elaborate cofactors to be used in combination with PEO. The synergism between PEO and other compounds is explained to be caused by hydrogen bonding and hydrophobic interaction, as explained in the precedent section. One of the first cofactor addition was done in a mineral flottation study [26]. Hydrophilic minerals like copper were treated with different types of surface modifiers to rend the minerals more hydrophobic. The flocculation of the suspension with PEO was then successful. Here, both of hydrogen bonding from the oxygen and the hydrophobicity from the ether groups of PEO, are thought to contribute to the flocculation process [26, 29].

Adding cofactors was found to be more effective in pulp suspensions as well as in mineral suspensions. In some cases, the use of cofactors is essential to the flocculation: it was also found that even with a very high degree of polymerization of PEO, poor retention of TiO_2 pigments was achieved since the polymer was not adsorbing both onto cellulose and pigments [28].

Other cofactors were also tested for interaction with the PEO chains: tannic acid [51, 52]; sulfonated [23] and non-sulfonated phenolic resins [22, 24, 43, 50, 62]; lignin derivatives [3, 23, 43, 53]; black liquor [25]; pectin [25]; carboxymethylcellulose [23]; acidic componds [43]; and alum [4, 43, 48, 49, 54]. Association of PEO with bentonite [49] activated fillers [50], and clay [55, 56] were tried. The flocculation efficiency was measured as a function of several parameters: zeta-potential [48]; temperature [4, 44]; pH [4, 48] as well as shear rate [24, 44, 47].

Of all the cofactors used, the phenolic resin (PR) compounds are very efficient in improving retion with PEO and seems to be the most widely used. The PEO/PR association has been studied in more details [57-58].

4.3 Flocculation mechanisms

Despite several findings on the synergism between PEO and various cofactors, the detailed mechanism involved has still not been fully established. As mentioned previously, the simple bridging mechanism, where two colloids are bridged by polymer molecules, was first proposed. This mechanism is unlikely to happen since in some systems, the PEO does not adsorb on the fibers or on fillers. For example deposition of clay particles onto fibers happens when PEO and sulphonated kraft lignin are added to the suspension, while none of these components adsorbs onto fibers [3]. The bridging mechanism was discussed again in 1987 by Leung and Goddard [43], but retention with PEO was found more effective when the pulp fibers were pretreated with aluminum species. They proposed a modified bridging mechanism where the aluminum species create a bridge between the fibers and the cofactor that is initially not adsorbing onto the fibers.

Lindström and Glad-Nordmark [5, 52], in 1984, argued that bridging mechanism was impossible and proposed instead the formation of a transient network. Latex removal from the bulk solution in a pulp fiber suspension was achieved. Again the simple bridging mechanism was unlikely to happen since neither PEO nor PR were adsorbing onto fibers. How removal of latex particles from bulk solution was then possible? They proposed a mechanism where the latex particles were intercepted in a three-dimensional hydrogen-bonded network formed by interaction between PEO and PR. There is a synergistic effect between PEO, PR and fibres for a critical order of addition. It is happening immediately after PEO and PR are mixed together. Polymer networks formed at low polymer concentrations are unstable. The transient nature (flocs break up) of this network requires the presence of cellulose fibers (collectors) at the formation to achieve latex removal. The role of the fibers is to sweep the transient network, collecting the particles before the network breaks apart. Also a fractionation effect was found on a latex suspension equally composed of 0.945 µm and 0.085 µm (in diameter). Close to the total amount of smaller particles stayed in the suspension while the bigger were entrapped in the proposed network.

Van de Ven and Alince argued against the network mechanism, and instead proposed the mechanism of association-induced polymer bridging [3]. The most compelling effect for the network mechanism is the fractionation of the latexes. In colloidal suspensions, larger particles are preferentially deposited onto a surface. Dynamic light scattering experiments suggested that sulphonated kraft lignin (KL), an other cofactor, is rending the PEO more soluble by decreasing the clusters size, giving no evidence for network formation. Two experiments are resumed here to illustrate the association-induced polymer bridging mechanism.

The adsorption of precipitated calcium carbonate (PCC) on fibres was tested. PCC carries positive charges and readily adsorbs on fibres which are negatively charged. When KL was added to the PCC suspension, the stability increased (no flocculation). This is caused by the negative KL molecules adsorbed on the PCC particles causing electrostatic repulsion. When the same experiment is performed in the presence of PEO and large concentration of KL, the deposition and flocculation kinetics are maximum at a PEO addition of 5 mg/g of PCC. This corresponds to 50% coverage of the PCC particles by the PEO. At KL concentration greater than a critical value, association-induced polymer adsorption and bridging occurs, and at very high PEO concentration, steric stabilisation happen.

The second set of experiments, on clay retention, gave the following results. Clay particles carry negative charges and do not adsorb onto fibres. When PEO is added to a clayfibre suspension, a transient flocculation appears. This suggests that PEO bridges the clay particles and fibres under the condition $\kappa\delta>1$. κ^{-1} is Debye length and δ is the thickness of the adsorbed polymer layer. But PEO itself does not adsorb onto fibres, apparently refuting the bridging mechanism. Filler-induced polymer bridging is evoked as an explanation in this case. The transient behaviour is explained by flattening of the polymer chains. If KL is added prior to PEO, the flocculation becomes permanent. This is explained by the stiffening of PEO chains by KL, preventing or minimising flattening.

The results of these experiments are based on the following theory. Adsorption of a cofactor on a polymer chain has a stiffening effect. For flexible water-soluble molecules, adsorption on a surface occurs when the energy of adsorption per polymer segment, χ_S, exceeds a critical value, χ_S^{crit} which is about 0.3 kT units [3]. For stiffer polymers the critical adsorption energy is less. The reason is that stiff polymers loose less entropy on adsorption than flexible ones, since they have fewer polymer configurations available to them. An infinitely stiff chain behaves as a rigid rod and no changes in entropy occurs on adsorption. For stiff polymers, χ_S^{crit} typically decreases to about 0.1 kT. The stiffer a polymer molecule is, the lower the energy required for adsorption. The synergistic effect of PEO/cofactor adsorbing onto a surface is called association-induced polymer adsorption. When the modified PEO chains bridge two particles, this is called association-induced polymer bridging.

The two proposed ways a cofactor can induce polymer adsorption and bridging are presented in Figure 8. The first schematic illustrates a flexible chain that does not adsorb onto fibers. The second is a stiffened chain by association, adsorption and bridging can occur. The same result can be obained when a cofactor is contracting a PEO chain instead of stiffening it. In that case, the number of configurations available to the PEO chain is also less, and the same theory for association-induced polymer adsorption and bridging applies. An example of such a cofactor is the modified phenolic resin (MPR,) presented in chapter II.

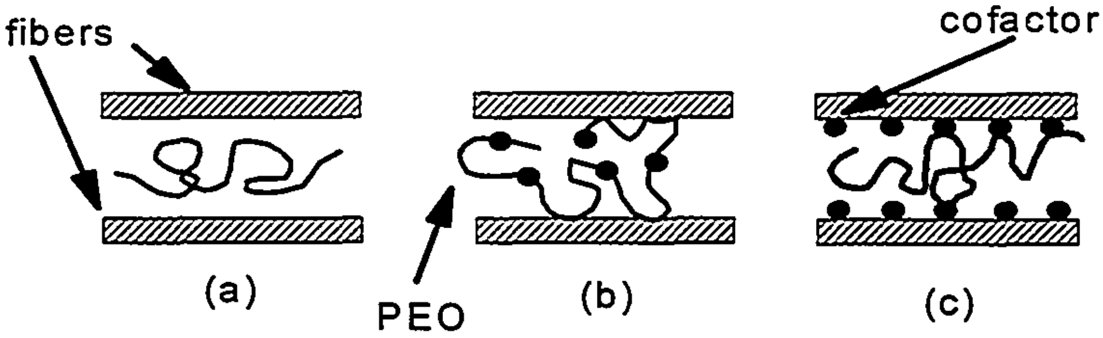

Figure 8: Schematics of association-induced polymer bridging. (a) Flexible polymer chain not adsorbing onto fibers. (b) Stiffened chain by a cofactor can adsorb onto a surface and bridge two fibers. (c) The polymer chain is bridged to the fibers surface by the already adsorbed cofactors, leading to a bridging of the fibers.

The third schematic represents association-induced polymer bridging when a PEO chain is linked to a surface by the cofactor. In that particular case, the cofactor should adsorb onto the fibers and is then acting as a dispersant. From the overview of PEO properties, mill applications, and the proposed mechanisms, this polymer seems to behave very differently depending on which cofactor or pulp constituant is in contact with. However, the association-induced polymer bridging is the more general, includes the exceptions, and possesses better thermodynamic and hydrodynamic fundations. To elucidate the possible mechanisms with cofactors that have not been studied yet, two apparatus using light as a probe were used. The light scattering theory is presented thereafter.

5.0 Light scattering

Electromagnetic radiation is one of the most important probes to the structure and dynamics of matter [59]. These radiations are basically described by Maxwell's equations. Light is hardly ever observed directly from its source. When looking at an object, a house for example, one sees scattered sunlight. *Extinction* or the lost in intensity of an incident light beam passing through matter. This is caused by *scattering* and *absorption* [60].

$$Extinction = scattering + absorption \qquad \textbf{(38)}$$

If light passes through a perfectly homogeneous medium, no scattering occurs. But, of course inhomogeneities are always present, and depending on the scale of these defects, light is more or less scattered. In this section, the general theory (Mie theory) about a spherical particle of any size is presented. Also two samplified models, Rayleigh and Rayleigh-Debye-Gans, are presented for their useful results.

Lets first define a system where light is scattered by an object. In Figure 9, the light beam is heading in the positive direction of the z-axis. I_{0V} and I_{0H} are the incident vertically and horizontally polarized light intensities respectively. The scatterer is located at the origin of the vertical xy-plane, and the scattered light impinges the observer located at an angle θ from the beam trajectory in the horizontal yz-plane.

The exact solution of the scattering of an electromagnetic wave by an isotropic, homogeneous sphere of arbitrary size, was formulated by Mie in 1908. The demonstration of the solution is quite laborious. Only the scattered intensity, I_V, from an incident vertically polarized wave is shown [61]:

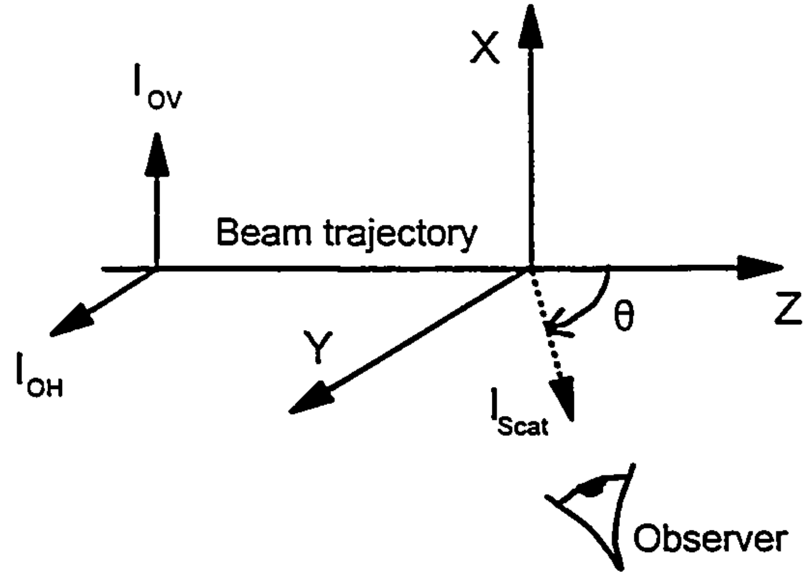

Figure 9: Diagram of scattered light to an observer from a given beam trajectory.

$$I_V = \left(\frac{\lambda_0^2}{4\pi^2 m_2^2 r^2} \right) i_V \tag{39}$$

where λ_0 is the indident wavelength in vacuum, m_2 is the refractive index of the medium, r is the distance between the scatterer and the observer, and i_V is called the intensity function for the vertically polarized light [61]:

$$i_V = S_V^2 \tag{40}$$

and,

$$S_V = \sum_{n=1}^{\infty} \frac{2n+1}{n(n+1)}\left(a_n \pi_n \cos\theta + b_n \tau_n \cos\theta\right) \tag{41}$$

where π_n and τ_n are Legendre functions and a_n and b_n are scattering coefficients which are functions of the particle size. The reader is referred to Kerker [61] for more details. The result is somewhat hard to interpret, and two simplifications of this important result are easier to visualise.

Prior to Mie, Rayleigh contributed to a simpler theory. It applies when the molecules or particles are of negligible size compared to the wavelength. The criteria is $a \ll \lambda_0/m_2$. Depending of the polarization of the incident beam (horizontal, H, or vertical, V), the scattered intensity is differing [61]. An unpolarized incident wave can be seen as the combination of the two incoherent linearly polarized components, vertical and horizontal. The scattered light, I_U, from an unpolarized beam is,

$$I_U = \frac{I_H + I_V}{2} = \frac{8\pi^4 a^6}{r^2 \lambda^4}\left(\frac{m^2-1}{m^2+2}\right)^2 (1+\cos^2\theta) \tag{42}$$

where a is the radius of the particle; m is the relative refractive index, m_1/m_2; λ is the wavelenght in the medium. It should be noted that the intensity goes as the sixth power of the particle radius and it falls as the square of the distance to the observer. Intensities of the incident wave are shown for vertical and horizontal polarization. The scattered intensity is schematically depicted in the Figure 10 as a function of the observer position, θ, in the horizontal plane. This pattern can be rotated to obtain a body of revolution. The Rayleigh scattering theory predicts the complete polarization of an unpolarized incident wave, I_{uo}, at 90 degrees.

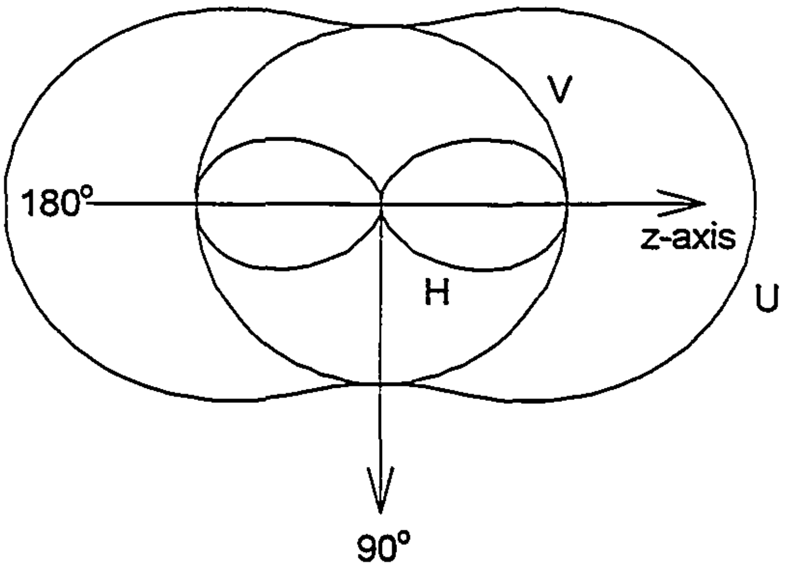

Figure 10: Radiations diagram for Rayleigh scattering. The circle represents scattered intensity from vertically (V) polarized light. The inner curve is for horizontally (H) polarized and outer one for unpolarized (U) light beam.

Another method was derived for particle sizes comparable to the wavelength of the latter probe. This is the Rayleigh-Debye-Gans scattering theory. The present case applies to, $a \ll \lambda_0/(2\pi m_2(m^2-1))$, for a particle of arbitrary shape, subdivided into volume elements.

Each volume element is assumed to respond to incident field, following Rayleigh scattering. The total contribution, I_T, of these scatterers (volume elements) equals to [61],

$$I_T = I_U \; P(\theta) \tag{43}$$

Where $P(\theta)$ is called the form factor, which for spheres is defined below.

$$P(\theta) = \left(\frac{3}{u^3} (\sin u - u \cos u) \right)^2 \tag{44}$$

Where u is defined as,

$$u = 2\zeta \sin\left(\frac{\theta}{2} \right) \tag{45}$$

and,

$$\zeta = \frac{2\pi a}{\lambda} \tag{46}$$

The important result from this form factor is that it weights the smaller particles more at large scattering angles. The reverse is right for larger particles.

Light scattering is a very efficient probe for colloidal suspensions. The elaborated theory for a spherical particle exists but simplified versions are useful for a better understanding of the particle size and scattering effects.

6.0 CONCLUDING REMARKS

Fines are difficultly introduced in the paper web. Water soluble polymers referred to as retention aids, are therefore necessary to achieve this task. The stability of a suspension is often perturbed by adding polymers. Polymer characteristics such as molecular weight, radius of gyration, and spatial extention of an adsorbed polymer chain are described. Their adsorption onto colloids can be explained via three concepts: hydrogen bonding, DLVO theory and free energy change. A modified Langmuir isotherm equation best illustrates the importance of the hydrodynamic conditions, and physicochemical properties of the colloids or polymers.

Polyethylene oxide (PEO) is a most effective retention aid widely used in papermaking. This neutral polymer is less sensitive than polyelectrolytes. However, in spite of years of industrial use, the mechanism by which PEO retains the colloidal particles onto the pulp fibers is still poorly understood. It is the objective of the present thesis to elucidate the synergistic adsorption mechanism of the system PEO/cofactor.

The hypothesis investigated is that flocculation happens via the association-induced polymer bridging mechanism. This mechanism is based on the principle that a freely dissolved PEO molecule is more easily adsorbed onto a collector when its configuration has been modified by a cofactor. However this mechanism is very general and properties of PEO in presence of a cofactor should be found for each cofactor. The following chapters are concerned with fundamentals such as: can PEO and cofactor adsorb onto the particles (latex and fines)? Are the PEO chains modified by the cofactor? Is the cofactor adsorb onto the particles or the PEO chains first?

7.0 REFERENCES

1- Smook, G.A., *Handbook for pulp and paper technologists*, CPPA, (1984).

2- van de Ven, T.G.M., *Nordic Pulp Pap. Res. J.*, 1, (1993),130-134,147.

3- van de Ven, T.G.M., Alince, B., *J. Pulp Pap. Sci.*, (in press).

4- Pelton, R.H., Allen, L.H., Nugent, H.M., Svensk Paperstidn., 9, (1980), 251-258.

5- Lindström, T., Glad-Nordmark, G., *J. Colloid Interface Sci.*, 97, 1, (1984), 62-67.

6 - van de Ven, T.G.M., *Colloidal hydrodynamics*, Academic Press, London, (1989) ch. 1,2.

7- Russel, W.B., Saville, D.A., Schowalter, W.R., *Colloidal dispersions*, Cambridge University press inc., (1989) ch. 8.

8- Hunter, R.J., *Foundations of colloidal science*, vol. 1. Oxford University Press, (1987) ch. 1-8.

9- Schumacher, G.A., Ph.D. Thesis, McGill Univ., Montreal (1990)ch. 1.

10- Fennel Evans, D., Wennerström, *H., The colloidal domain where physics, chemistry, biology, and technology meet*, VCH Publishers Inc., (1994) ch. 7, 8.

11- Hiemenz, P.C., *Principles of colloid and surface chemistry*, Marcel Dekker inc., (1977) ch. 9, 10.

12- Voyutsky, *S., Colloid chemistry*, Ed. Mir publishers, (1978)ch.1-3, 9.

13- Kamiti, M., Ph.D. Thesis, McGill Univ., Montreal (1994)ch.1.

14- Napper, D.H. *Polymeric stabilization of colloidal dispersions*, Academic press inc., (1983) ch. 1-5.

15- Hiemenz, P.C., *Polymer chemistry*, Marcel Dekker inc., (1984)ch. 1,2,4,9,10.

16- Yamakawa, *H., Modern theory of polymer solutions*, Harper & Row publishers inc., (1971).

17- Dewitt, J.A., van de Ven, T.G.M., *Adv. Colloid Interface Sci.*, 42, (1992), 41-64.

18- De Gennes, P.-G., *Scaling concepts in polymer physics*, Corneli University press, (1979).

19- van de Ven, T.G.M., *Adv. Colloid Interface Sci.*, 48 (1994) 121-140.

20- Kamiti, M., van de Ven, T.G.M., *J. Pulp Pap Sci.*, 20, 7, (1994), J199-205.

21- Molyneux, P., *Water-soluble synthetic polymers: properties and behavior*, I, CRC Press (1984)

22- Chan. L.L., *CPPA Annual Mtg.*, (Montreal), 69B (1983) 9.

23- Pelton, R.H., Allen, L.H., Nugent, H.M., *Tappi J.*, 64, 11, (1981), 89-92.

24- Stack, K.R., Dunn, L.A., Roberts, N.K., *Appita*, 43, 2, (1990), 125-129.

25- Rahman, L., Tay, C.H., *Tappi Papermakers conf.*, (New Orleans), (1986), 189-198.

26- Rubio, J., *Colloids Surfaces*, 3, (1981), 79-95.

27- Stack, K.R., Dunn, L.A., Roberts, N.K., *J. Wood Chem. Tech.*, 13, 2, (1993), 283-308.

28- Howard, G.J., Lyth Hudson, F., West, J., *J. Applied Poly. Sci.*, 21, (1977), 45-54.

29- Lindström, T., Glad-Nordmark, G., *J. Colloid Interface Sci.*, 94, 2, (1983), 404-411.

30- Lindström, T., Glad-Nordmark, G., *Svensk Paperstidn.*, 15, (1978), 489-492.

31- Kondo, T., Sawatari, C., *Polymer*, 35, 20, (1994), 4423-4428.

32- McGary, C.W. Jr, *J. Polymer Sci.*, XLVI, (1960), 51-57.

33- Minoura, Y., Kasuya, T., Kawamura, S., Nakano, A., *J. Polymer Sci.*, A-2, 5, (1967), 125-142.

34- Polverari, M., van de Ven, T.G.M., *J. Phys. Chem.* (In press).

35- Pelton, R., *Nordic Pulp Pap. Res. J.*, 1, (1993), 113-119.

36- Petlicki, J., van de Ven, T.G.M., *Colloids Surfaces*, 83, (1994), 9-23.

37- Petlicki, J., van de Ven, T.G.M., *J. Pulp Pap. Sci.*, 20, 12, (1994), 375-382.

38- Couture, L., van de Ven, T.G.M., *Colloids Surfaces*, 54,(1991), 245-260.

39- Polverari, M., van de Ven, T.G.M., *Colloids Surfaces*, 86, (1994), 209-228.

40- Dewitt, J.A., van de Ven, T.G.M., *Colloids Surfaces*, 66, (1992), 227-230.

41- Polverari, M., van de Ven, T.G.M., *J. Colloid Interface Sci.*, 173, (1995), 343-353.

42- van de Ven, T.G.M., *Colloids Surfaces*., 39,(1989), 107-126.

43- Leung, P.S., Goddard, E.D., *Tappi J.*, 70, 7, (1987), 115-118.

44- Lindsay, B., *Paper* (London), 203, 9, (1985), 14-17.

45- Carrard, J., Pummer, H., *U.S. Patent*, 4, 070 (1978) 236.

46- Pelton, R.H., Allen, L.H., Nugent, H.M., *U.S. Patent*, 4, 313 (1982) 790.

47- Brine, S.R., Brauer, R.M., Wiseman, N., *Appita*, 45, 2, (1992).

48- Tay, C.H., *Tappi J.*, 63, 6, (1980), 63-66.

49- Rahman, L., *Advanced topics in wet-end chem.* Short course, Tappi notes, (1989), 39-51.

50- Tay, C.H., Cauley, T.A., *Tappi Papermakers Conf.*, (Atlanta), (1982), 205-210.

51- Attia, Y.A., Rubio, J., *Br. Polym. J.*, 7, (1975), 135-138.

52- Lindström, T., Glad-Nordmark, G., *Colloids Surfaces*, 8, (1984), 337-351.

53- Picaro, T., van de Ven, T.G.M., *J. Pulp Pap. Sci.*, 21, 1, (1995), 13-18.

54- Stack, K.R., Dunn, L.A., Maughan, S., *Appita*, 48, 4, (1995), 275-283.

55- Lapčik, L., Alince, B., van de Ven, T.G.M., *J. Pulp Pap. Sci.*, 21, 1, (1995), 19-24.

56- Roick, G.T., Lloyd, J.A., *Appita*, 47, 1, (1994), 55-58.

57- Stack, K.R., Dunn, L.A., Roberts, N.K., *Colloids Surfaces*, 61, (1991), 205-218.

58- Lindstrom, T., *Sepn Sci. Technol.*, 14, 7, (1979), 601-610.

59- Berne, B.J., Pecora, *R., Dynamic light scattering, with applications to chemistry, biolofy & phisics*, John Wiley & Sons inc., (1976)ch.1-3.

60- van de Hulst, H.C., *Light scattering by small particles*, John Wiley & Sons inc., (1957).

61- Kerker, *M., The scattering of lightr and other electromagnetic radiations*, Academic press, (1969)ch.1-3,8.

62- Xiao, H., Pelton, R., Hamielec, A., *J. Polymer Sci.*, A, 33, (1995), 2605-2612.

CHAPTER II

DYNAMIC LIGHT SCATTERING OF PEO SOLUTIONS AND SUSPENSIONS OF PEO-COATED LATEX PARTICLES

1.0 INTRODUCTION

Our primary motivation to study the cofactors (sodium naphthalene sulphonate, carbamide, and modified phenolic resin) effects on polyethylene oxide (PEO) with the dynamic light scattering technique, was to see whether they change PEO chain configurations or not [1]. This technique might be useful to understand why the cofactors, used in retaining colloidal matter on a paper machine fabric, have different efficiencies.

The PEO has been extensively studied in the past. A great amount of literature on the interaction of PEO with other chemicals called cofactors was found. Notably on compounds like carbamide and phenolic resins. Most of researchers agree on a hydrogen bonding between a cofactor molecule and a PEO chain, but controversy about the flocculation mechanism is still existing.

The technique of dynamic light scattering (DLS) has been proved efficient in measuring the layer of polymer adsorption onto latex particles as well as measuring the free coil Stokes diameter of polymers. Therefore, the change in PEO characteristics due to the addition of a second component, a cofactor, can be measured.

In other words, adding a cofactor to PEO in solutions or suspensions, will bring the results to deviate, giving some indices on the flocculation mechanism.

The development of this chapter starts with a detailed section of the experimental part of the project. The preparation of the solutions and suspensions, with the chemicals and the latex particles, is described. A description of the apparatus (photon correlation spectroscopy), is given as well as the procedures followed to take the measurements.

The results and discussion section starts with the PEO solution as a one or two-component system. This section was done to see if the cofactors were interacting with PEO. The last section was done on a two or three-component system: the latex particles, the PEO, and the cofactors. Completing the precedent part, these experiments were also simulating a pulp suspension where the wood fibers were represented by latex spheres.

2.0 EXPERIMENTAL

2.1 Materials

The polymer and cofactors were provided by E.QU.I.P. International Inc. (Baie d'Urfé, Québec, Canada). The neutral polymer used is a polyethylene oxide of a number-average molecular weight, M_N, of 2 millions with a polydispersity of about 3.5, giving a weight-average molecular weight, M_W, of 7 millions. The cofactors used were of three types: the first one contains a reactive called sodium naphthalene sulphonate, and will subsequently be called SNS; the second one contains carbamide, CAR; and the third one is a modified phenol-formaldehyde resin, called MPR.

The latex used was one of the sample, L-3, described in [2] by Polverari and van de Ven. It was obtained from BASF Corporation (Sarnia, Ontario, Canada). It is made of 100% styrene with SO_4^{2-} functional surface acid groups.

2.2 Solutions and suspensions preparation

Freshly distilled, deionized, filtered water was used to prepare aqueous PEO solutions and suspensions. A chromatographic filter of 0.2 µm was used in filtration. All glassware was cleaned with potassium dichromate acid solution, followed by rinsing in distilled, deionized, filtered water. Fresh PEO stock solutions were prepared at a concentration of 2 g/L, previously to each experiment. The PEO solutions were stirred for 24 hours to completely dissolve the polymer and then put aside for another 24 hours without stirring before using it.

The solid content of the latex stock suspension was 0.00254% for a particle concentration of $1.1 \cdot 10^{10}$ particles/mL for a total available surface for adsorption of $9.10 \cdot 10^{4}$ m^2/mL.

Cofactors stock solutions of 6 g/L were freshly prepared previously to each experiment from aqueous commercial samples. These commercial samples were highly concentrated (nearly 50% consistency). To make up the samples to be measured by photon correlation spectroscopy (PCS,) the chemicals were diluted to the desired concentration into a scattering cell of 1.2 cm in diameter. The dilution water was always added before the chemicals. All stock solutions and dilution water were filtered again through a 0.2 μm chromatographic filter, and the latex stock suspension through a 0.45 μm filter. Between each chemical addition, the sample cell was gently shaken and ultrasonicated for 15 seconds. The chemical ratio (weight of commercial solution / weight of dry PEO (g/g),) was varied. The sequence of chemical addition has also been varied and found to be very important in some cases. The prepared sample cell was introduced in the temperature controlled bath of the goniometer. Measurements were taken 15 minutes after the addition of the last chemical (defined as sample aging time).

2.3 Instrumentation and analysis

Dynamic light scattering [3-7] experiments were made using a vertically polarised He-Ne laser manufactured by SpectraPhysics, with a light beam of a wavelength of 632.8 nm. A photon correlation spectrometer (Brookhaven Instruments BI-2030) with a (64 + 8) channel, 6 bit autocorrelator was used with its original integrated optics to measure the scattered light at 90°. Only scattered light was allowed to impinge on the photomultiplier tube (homodyne detection). A refractive index matching bath of filtered (0.2 μm) decalin surrounded the scattering cell, and its temperature was controlled to 25±0.1°C. A description of the apparatus and basic theory is given in appendix A.

2.3.1 Polymer solutions measurements

Before any experimental measurement, it is possible to calculate theoretical polymer dimensions in solution. The RMS end-to-end distance, $< r^2 >^{1/2}$, for a non interacting PEO chain molecule can be calculated [8]. This so called unperturbed dimension represents the short range interactions such as bond angle restrictions and steric hindrances to internal rotation.

$$<r^2>^{1/2}\ (nm) = (750 \pm 30) \cdot 10^{-4} \cdot M^{1/2} \tag{1}$$

where M is the molecular weight, assuming a polydispersity of 1. A value of 106 nm is obtained for a M_N of $7 \cdot 10^6$. An important relation between the RMS end-to-end distance and the radius of gyration, R_g, is given in [9]:

$$R_g = \frac{<r^2>^{1/2}}{6^{1/2}} \tag{2}$$

which is equal to 43.3 nm in the present case. Assuming Gaussian distribution in molecular weight, for a polydisperse polymer sample, the theoretical Stokes radius, R_S, is given by [10]:

$$R_S = 0.676\ R_g \left(1 + \left(\frac{M_W}{M_N} - 1\right)^{1/2}\right)^{1/2} \tag{3}$$

where M_W and M_N are the weight and number-average molecular weights respectively. A

Stokes radius of 47 nm was obtained, giving a polymer free coil diameter of 94 nm.

Once the sample cell introduced in the goniometer, measurements were taken. The free coil hydrodynamic diameter (Stokes diameter) was determined using the cumulant method (eq. 5). This method was chosen due to the polydispersity of the industrial PEO. For polydisperse systems, the average linewith, Γ, is given by:

$$\bar{\Gamma} = \int \Gamma \, G(\Gamma) \, d\Gamma \tag{4}$$

where G(Γ) is the normalized distribution in Γ values. The normalised homodyne autocorrelation for a polydisperse suspension is then expressed as:

$$g^{(2)}(\tau) = 1 + e^{-2\bar{\Gamma}\tau} \left(1 + \frac{1}{2} \mu_2 \tau^2 - \frac{1}{6} \mu_3 \tau^3 + \ldots \right)^2 \tag{5}$$

where μ_i is the i^th^ moment of the distribution and τ is the sample time. The linewidth Γ, is:

$$\bar{\Gamma} = \bar{D} \, q^2 \tag{6}$$

where the diffusion coefficient is:

$$\bar{D} = \frac{kT}{6\pi\eta\bar{a}} \tag{7}$$

The average particle radius, $\bar{a}$, can be calculated by introducing the thermal energy, kT, and the viscosity, η, of the solvent into equation (7). The definition of the scattering vector, q, is:

$$q = \frac{4\pi m_2}{\lambda_o} \sin\left(\frac{\theta}{2}\right) \tag{8}$$

where m_2 is the index of refraction of the suspending medium, λ_o is the wavelength of the incident beam in vacuum, and θ is the scattering angle.

In Dynamic Light Scattering, it is very important to know if the particles in suspension are highly interacting. A simple calculation to quantify this is derived here. Different concentration regimes must be distinguished to describe a polymer solution: concentrated, semidilute and dilute state [11]. The crossover between dilute and semi-dilute can be taken as when the volume of all polymer coils together is equal to the volume of the solution. The volume of a single polymer coil is:

$$V_{Coil} = \frac{4}{3} \pi R_g^3 \tag{9}$$

Using this equation, the volume of a coil (at $R_g = 43.3$ nm), is equal to $340 \cdot 10^{-24}$ m^3. A total of $2.94 \cdot 10^{18}$ coils are required to fill one litre. The crossover happens at 9.8 g/L for a M_N of $2 \cdot 10^6$. All the solutions studied were at 250 mg/L. The system was thus always in the dilute regime.

2.3.2 Latex particles suspension measurements

An other set of experiments was done to find the thickness of adsorbed polymer layer onto a collector which is in the present case, latex particles. The cumulant method was used to obtain the average diameter of the particles in the sample cells. The hydrodynamic layer thickness, δ_H, was calculated in the following way:

$$\delta_H = a_{PEO} - a_{bare} \tag{10}$$

where a_{bare} and a_{PEO} are the hydrodynamic radius of the bare and PEO-coated latex particles respectively. The sequence of addition was found to be critical when a cofactor and PEO were introduced into a latex suspension.

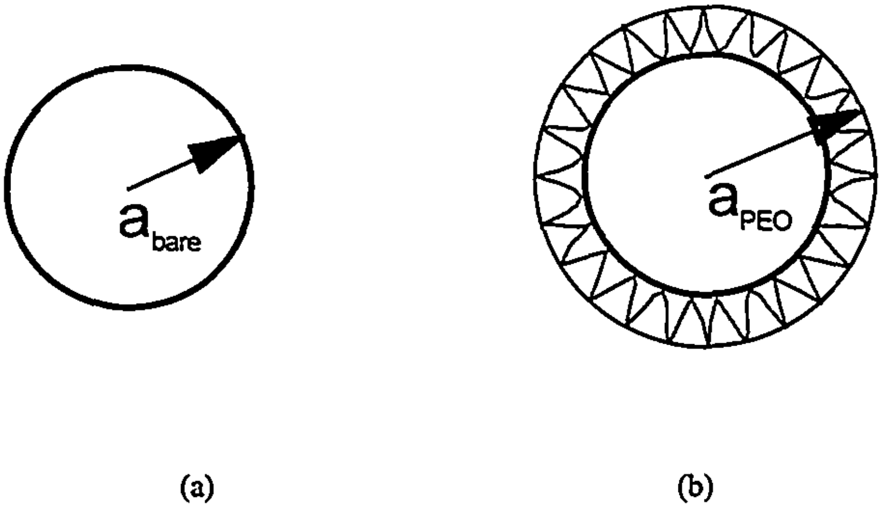

Figure 2.1: The hydrodynamic layer thickness, (HLT), is the thickness of the adsorbed polymer onto a latex particle. The radius of the bare latex particles, (a), is measured prior to the PEO-coated latex particles (b).

2.3.3 Relative concentrations

The amount of PEO required to coat a latex particle was determined after the experimental layer thickness plateau obtained by Polverari and van de Ven [2]. For a filtered PEO sample of M_w $5.72 \cdot 10^5$, the plateau was reached at a relative concentration of 1000 mg of PEO/m^2 of latex. The chosen relative concentration was of 1250 mg of PEO/m^2 of latex. Full coverage of the latex particles is attained ahead of the plateau. The specific adsorption is usually of the order of 1 mg PEO/m^2.

It is also relevant to calculate the approximative amount of cofactor (on a dry basis.) added to the latex suspension. In the case of a high affinity between the cofactor and the latex particles, the specific adsorption for the cofactors is expected to be of the order of 0.1 mg/m^2 of latex. Table I, suggests that if a cofactor is to adsorb onto latex particles, full coverage will happen, even at a chemical ratio (cofactor / PEO) of 1 to 1.

Table I: Approximative amount of dry cofactor per square meter of latex, as a function of the chemical ratio, for [PEO] = 250 mg/L.

Ratio (Cofactor / PEO)*	Dry mass** of cofactor(mg)/m^2 latex
1/1	625
3/1	1880
5/1	3120
10/1	6250

* The ratio is the relative volume (ml) of the concentrated commercial sample to the weight (g) of the dry PEO.

** Approximative value based on 50% solids.

3.0 RESULTS AND DISCUSSION

3.1 Polyethylene oxide solutions with and without a cofactor

This experiment was done to characterize the PEO used, and to find out if the cofactors are interacting with PEO chains and how these interactions are taking place. As described previously, PEO concentration was always held at 250 mg/L. When a cofactor was added to PEO solution, a chemical ratio (cofactor/PEO) of 3/1 was applied. The apparent diameter, the scattering intensity of the solution and the P-factor were taken simultaneously. The P-factor is a measure of the polydispersity of the sample, calculated from the cumulant method (eq. 2) as follows:

$$\text{P-factor} = \frac{\mu_2}{\bar{\Gamma}^2} \qquad (11)$$

where μ_2 and Γ are the second moment and the averaged linewith of equation (5).

The results of the PEO solutions are presented as bar charts in figures 2 and 3. Measurements were first done on PEO solutions when no cofactor was added. The value of 129 nm is higher than the theoretical Stokes diameter of 94 nm precedently calculated. The sample standard deviation, STDS, was of 19.1 nm on the first measurements. Polverari and van de Ven have also found that the average given by the cumulant method was bigger than the theoretical value, due to the presence of reforming clusters [10]. Although the sample were filtered with a 0.2 µm chromatographic filter, some cluster might have been introduced in the sample cell, and then contributed to the scattering of light.

The apparent diameter measurement on the sixth day (d-6) was not significantly different from the one taken at fifteen minutes (d-0), of sample aging.

On the other hand, the intensity changed significantly more than its sample standard deviation (STDS = 6.15%). The contribution of the darkcounts and the dilution water, to the photocounts were removed. No significant change in P-factor was observed. The magnitude of the standard deviations, for the apparent diameter and the intensity, are attributed to the polydispersity of the industrial PEO sample. The intensity increased by almost two fold between the two series (d-0 and d-6) from 3.0 to 5.8 respectively.

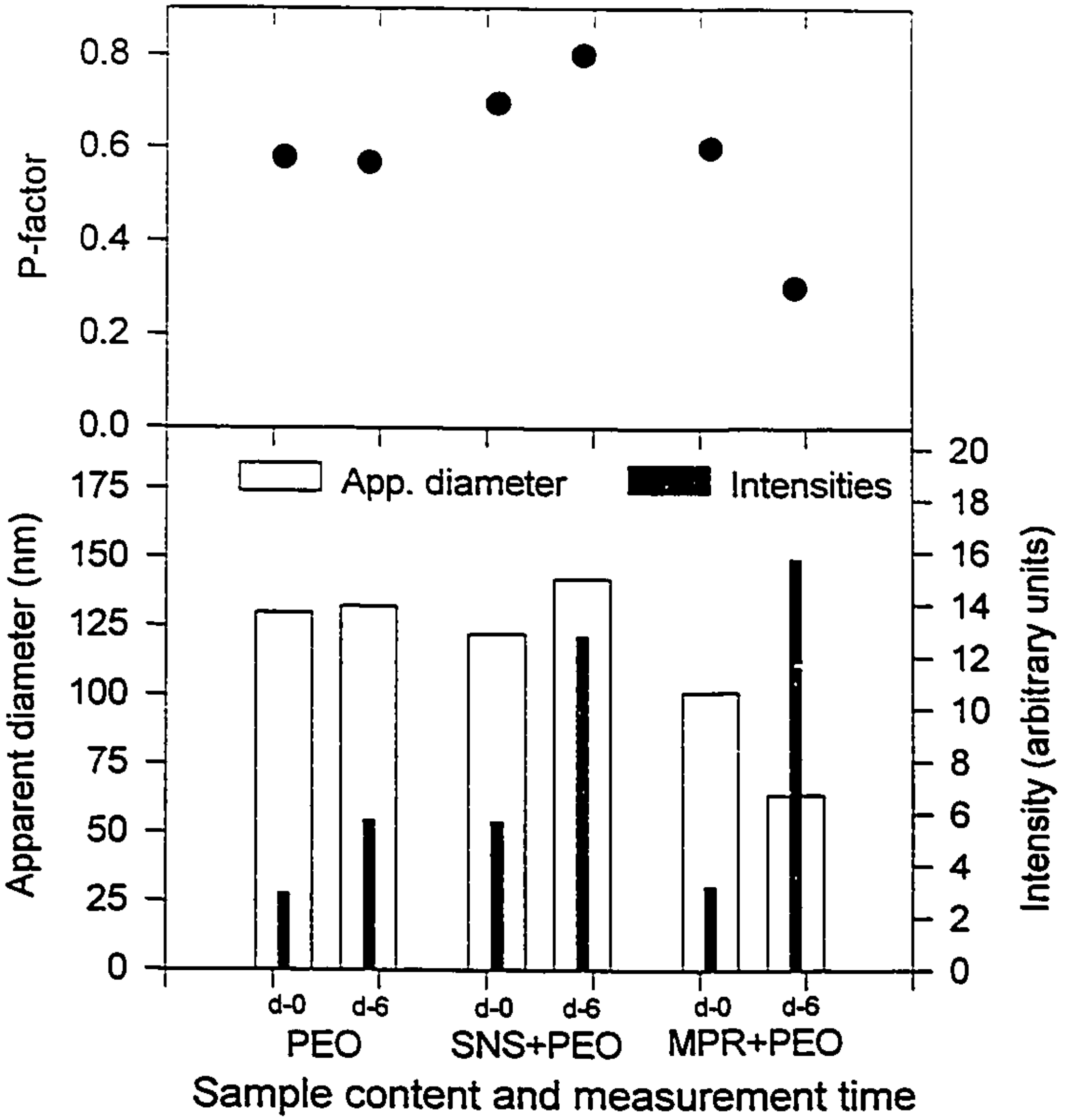

Figure 2: Solutions of PEO with and without cofactors. The upper graph represents the P-factor values from equation 11. In the lower graph, the empty boxes represent the apparent diameter and the filled boxes represent the scattered intensities from the polymer solutions. The measurements were taken 15 minutes (d-0,) and six days (d-6,) after sample preparation. [PEO]=250 mg/L, chemical ratio=3/1.

This increase is likely due to the reformation of clusters as proposed by Polverari and van de Ven [10]. The samples being filtered already contain a small quantity of clusters that continue to grow in number and size with time to reach a thermodynamic equilibrium. PEO solutions were found to be left with two particle fractions, the free coils and the clusters. The bigger diameter is the one of clusters that was found in [10] after a period of 6 days. It was 450 nm and found to be independent of the polymer molecular weight. Schumacher and van de Ven [12] used the normalized heterodyne autocorrelation for a well defined bimodal dispersion of latex spheres of different sizes, a_A and a_B. It was found in that the PCS data can be fitted to give two different particle sizes instead of an apparent diameter which is neither the one of the smaller nor of the bigger particles. The bimodal autocorrelation is:

$$g_{BI}^{(2)}(\tau)=1+\frac{I_A^2}{(I_A+I_B)^2}\,e^{(-2\Gamma_A\tau)}+\frac{2I_AI_B}{(I_A+I_B)^2}\,e^{(-\Gamma_A\tau)}\,e^{(-\Gamma_B\tau)}+\frac{I_B^2}{(I_A+I_B)^2}\,e^{(-2\Gamma_B\tau)} \qquad (12)$$

where I_A and I_B are the scattered intensities for the smallest and biggest sized particle fractions respectively. This equation is derived in appendix A. The four unknowns in the present case are a_A and a_B, I_A and I_B. In the present case, the smaller diameter is the free coil which is taken as the measurement immediately after PEO solution was made, 129 ± 19 nm, and 450 nm for the clusters. The particle size ratio 129 nm over 450 is very close to 0.291 which has been studied by Schumacher and van de Ven [12]. I_A is taken as the intensity measured at d-0 making the hypothesis of no clusters in the first half hour after filtration. I_B is taken as the difference in intensity from d-0 to the intensity at d-6. The decrease in I_A intensity due to the lower concentration of free coils at d-6 has been neglected. The value of $\log(I_B/I_A)$ was calculated and reported in figure 1 b) of [12]. A value of 1.8 was found for the dependant variable Γ_A / Γ. The sought linewith Γ_A is the one of the free coils only. On the other hand, the force fit Γ, is the one called apparent, from which the apparent diameters in figure 2 were calculated. The calculated free coil Γ_A was then used to obtain a new Stokes diameter, $2a_A$, of 72 nm. The difference between the apparent diameter at d-0 (129 nm) and the calculated value at d-6 is significant. Polverari and van de Ven found a coil diameter of 60 nm for a PEO M_w $5 \cdot 10^5$. The value of 72 nm seems to be low for its high molecular weight (by extrapolation,) but it can be due to a segregation of the shortest and longest chains. The longest ones are probably entrapped into clusters.

Addition of SNS

The addition of SNS to fresh PEO sample was studied. Both of the apparent diameters (SNS d-0 and d-6) did not change significantly from the value of PEO d-0 (within the STDS range of 19.1 nm). Thus, SNS does not have an effect on the apparent diameter, even over a six day period. But the P-factor (polydispersity factor,) had increased slightly from PEO, indicating that complexes or clusters, might be present. A complex is formed when a cofactor associates with PEO, but the PEO chains are still single. Further association between PEO/cofactor complexes, or between PEO molecules alone, leads to clusters formation. The biggest measured effect of adding this cofactor is seen in the scattered intensities of the solution. The contributions to the photocounts by the darkcounts, dilution water, and the cofactors, when it was added, were subtracted from both of d-0 and d-6 measurements. An apparent diameter of 15 nm was measured from SNS solutions (no PEO). The SNS is then probably present in a polymeric form. Napper [9] has given an approximation equation for many carbon backbone polymers. This can give us an idea of the molecular weight of the SNS. The end-to-end distance, $<r^2>^{1/2}$, is given by,

$$<r^2>^{1/2}(\mathrm{nm}) = 0.06\ M^{1/2} \qquad (13)$$

Using the equations (2) and (3), and assuming a polydispersity of 1, SNS molecular weight is approximately $2 \cdot 10^5$.

Compared to the PEO alone, the first series of measurements, (d-0), are 2 fold higher in intensity. This is evidence that not only complexes are formed but clusters of these complexes are also forming. The time (from d-0 to d-6) had contributed to a further increase in intensity by a factor of 2.2, most likely due to an increase in the number of clusters. The relative growth in time, from d-0 to d-6, is comparable to the case of PEO alone, 2.2 fold compared to 2 fold for PEO alone.

Addition of MPR

Measurements on MPR (alone) solutions have revealed a low intensity and no measurable particle diameter. The MPR could be a polymer [13] but it seems to be of a low molecular weight. For MPR+PEO solutions there is a significant decrease in both apparent diameters (d-0 and d-6). The time taken between the two measurements is contributing further to the decrease in the apparent diameter from d-0. An explanation for the smaller apparent diameter could be that the biggest chains are entrapped into the clusters and the apparent diameter is the one of the smallest free chains. The clusters being too big to be detected by the PCS at the given sample time. The other explanation is that the PEO/MPR complexes formed are taking a more and more compact configuration, giving a smaller apparent diameter. The intensity of MPR d-0, is slightly higher than PEO d-0 by only 7%. This might be an evidence that the formation of clusters is low. The freshly PEO/MPR solutions might be mainly constituted of PEO/MPR complexes and only a few clusters.

After 6 days, the intensity was at the highest value of all experiments. It is 5 fold higher than at d-0. The intensity increase is again a sign of cluster formation. From the decrease in the p-factor, it is also evident that the clusters and complexes are of small diameter. Xiao and Pelton [14], had confirmed the association of PEO and phenolic resins. Another study on the association of phenolic resins and PEO, done by Stack et al. [13], mentioned that some types of phenolic resins have the ability to contract the coils of PEO.

Addition of CAR

Shown in Figure 3, an enormous change in the apparent diameter of PEO is found immediately after addition of CAR which became larger with time. An apparent diameter of more than 2 µm gives no doubt about PEO/MPR complexes and clusters formation. Literature was also found about the formation of complexes between CAR and PEO [15-19].

Intensities at d-0 and d-6 are both lower than the intensity of PEO d-0. Like for the other cofactors, the scattered intensity from the CAR solution (without PEO), was subtracted from the mixture value. A relatively high intensity (7.3 a.u.) was measured for a fresh CAR solution. That is one reason why the intensities of CAR d-0 and d-6 are both lower than PEO d-0. An apparent diameter of 108 nm was measured and found to decrease with time. Also from visual observation, the commercial stock solution showed suspension behaviour, by scattering light. The CAR cofactor thus appears to behave more like a colloidal suspension [17], than a polymer solution. A heteroflocculation between the CAR and PEO is likely to happen, but it is difficult to know if the PEO chains and clusters are flocculated by CAR or if the CAR aggregates are flocculated by PEO chains. However, those low intensities and big apparent diameters can be due to a bridging of CAR colloids in a very loose structure.

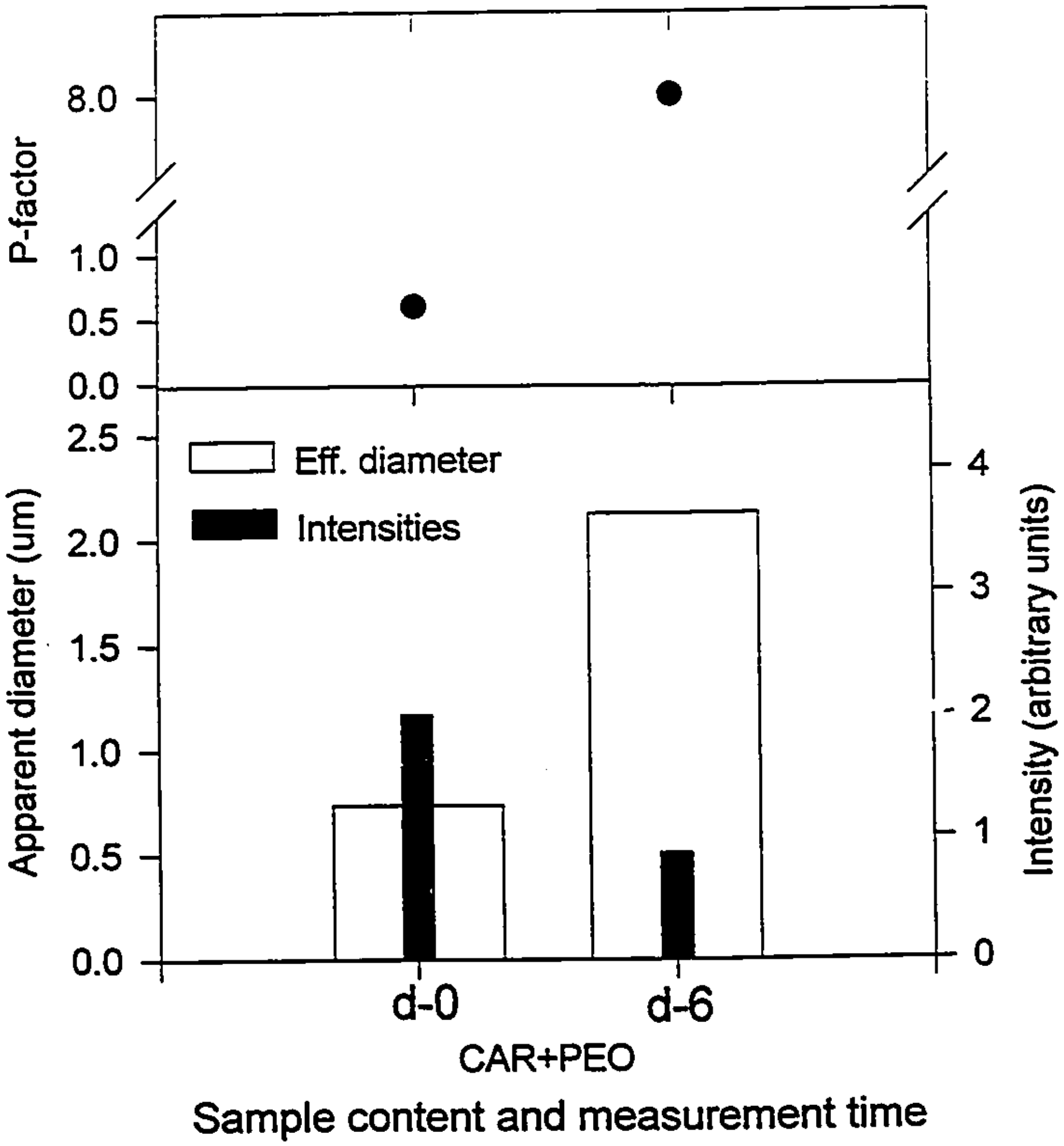

Figure 3: Solutions of PEO with CAR cofactor. The upper graph represents the P-factor values from equation 11. In the lower graph, the empty boxes represent the apparent diameter and the filled boxes represent the scattered intensities from the polymer solutions. The measurements were taken at 15 minutes (d-0,) and six days (d-6,) after sample preparation. [PEO]=250 mg/L, chemical ratio=3/1.

The P-factor becomes remarkably high after a period of 6 days. A segregation would have had the same effect if the longest PEO chains are entrapped into the clusters, leaving the smallest ones in solution [16]. An other possibility is that the cofactor was composed of more than one compound, thus creating two or more types of complexes after a long period of time.

3.2 The latex suspensions

PEO is known to adsorb onto latex particles. Adding a third component (cofactor) to the binary system latex-PEO may change the conformation of the PEO chains or the surface (active sites,) of the latex particles. The following section investigates these possibilities. The hydrodynamic layer thickness (HLT) of polymer adsorbed onto latex particles were measured. One of the first experiment made on latex suspension is shown in table II.

Table II: Hydrodynamic layer thickness (HLT) of PEO adsorbed onto latex particles, with and without cofactors. [PEO] = 250 mg/l, chemical ratio = 3/1. Sequence of addition, latex-cofactor-PEO (LCP).

	HLT (nm)	STDS HLT (nm)	P-factor
Latex (L)	0	2.7	0.2
L+PEO	73.8	4.9	0.22*
L+PEO+SNS	42.5	3.4	0.23
L+PEO+CAR	4.6	5.4	0.28
L+PEO+MPR	297.8	12.5	0.35

* STDS = 0.03

The latex particles diameter was measured (172 ± 2.7 nm,) and found to be in agreement with the previous value (169 nm) given by Pelverari and van de Ven [2]. A PEO layer thickness of 73.8 nm is obtained for an increase of only 0.02 in the P-factor as a sign of no flocculation. In the work from Polverari and van de Ven [2], for the latex L-3 in figure 5, extrapolation to a M_w of $7 \cdot 10^6$ gives a HLT of 114 nm. This value is of the same order of magnitude as the measured 73.8 nm, and is sufficiently close for such an extrapolation. The HLT value of 73.8 nm is higher than the ones obtained for lower M_w [2, 21].

The addition of a cofactor prior to the addition of PEO will change the surface of the latex particles if it does adsorb onto it. Following that the cofactors are known to interact with PEO (fig 2 and 3), association-induced polymer bridging can happen via two mechanisms: PEO/cofactor complexes, bridging two bare particles (when the cofactor does not adsorb onto the particles,) and PEO molecules bridging two cofactor-coated particles [1]. The figure 8 of chapter I depicts the difference between the two mechanisms. As previously discussed in table I, at a 3/1 chemical ratio, an excess of cofactor is likely to happen, keeping a great amount in solution.

Addition of SNS

Addition of SNS to the latex suspension had the effect of inhibiting the buildup of the layer of PEO to only 42.5 nm. The P-factor did not change significantly indicating that no flocculation occurred and the system is still relatively monodisperse. Does the SNS adsorb onto the latex particles or not? If the cofactor is adsorbing, the cofactor-coated particle may have less adsorption sites left for PEO chains. Also, SNS-coated latex particles may be more attractive for PEO and polymer flattening might occur at a higher degree or rate, preventing further adsorption of PEO chains.

As soon as the PEO is introduced into the sample cell, most of the adsorption sites on PEO molecules may become occupied by the cofactor molecules before association-induced polymer adsorption onto latex particles occurs. If the latex particles are already coated by SNS, an electrostatic repulsion might happen, keeping the layer thickness thinner. That could be an exception to the stiffening effect explained in [1].

Addition of CAR

When CAR was added to the suspension, no significant adsorption of PEO was found. The P-factor had increased slightly indicating that the system was less homogeneous. One possible explanation is that when the PEO is added, the PEO/CAR complexes stay in solution, giving no layer of adsorption. In reference [15], the combination of PEO with CAR, giving complexes, was found an excellent detergent in washing artificially soiled cotton. Then it might not be surprising that no significant PEO HLT on latex particles is found. The increase in P-factor can be due to the mixture of latex particles (172 nm) and big PEO/CAR complexes and clusters (735 nm,) measured in solution.

Addition of MPR

The third component, MPR, had increased the layer thickness and also the P-factor. MPR does change the configuration of the PEO chains, as seen in figure 2. The chains are thought to shrink in size. Since three layers of unmodified PEO chains on top of the other are required to obtain and equivalent HLT to the present one, more than that are likely required in the case of PEO/MPR complexes. Thus, clusters of PEO/MPR complexes might be formed in solution and then deposited on latex particles or simply formed at the surface of the particles. An other possible explanation for the thick HLT, can be that a slight flocculation occurred. In all cases, the P-factor is increased due to inhomogeneities in the adsorption process.

3.2.1 Sequence of addition

The variation of the sequence of addition of the chemicals has also been studied. The three sequences are LCP (latex-cofactor-PEO,) LPC (latex-PEO-cofactor,) and PCL (PEO-cofactor-latex). The results are presented in figure 4. The usual sequence of chemical addition seen in paper mills applications is LCP. In the sequence (LPC) two scenarios can happen depending on whether the cofactor does adsorb onto the latex particles or not. In the former case, the polymer added last will interact with cofactor-coated latex particles and cofactor molecules in solution. In the other case (no adsorption of the cofactor onto the particles,) all the cofactor will stay in solution. If the chemicals are added in the sequence LPC, the cofactor is forced to interact with the PEO chains which are coating the latex particles. The third sequence (PCL) was done in mixing the polymer and the cofactor prior to the addition of the latex suspension. Therefore they had more time to interact with each other.

Addition of SNS

No significant difference in HLT was found between the sequence LCP and PCL. The P-factor is somewhat increased in the latier sequence, indicating a system less monodisperse. In the latter sequence, the PEO/SNS clusters had more time to form before they were in contact with latex particles. Thus, they are probably the cause of the increasing in P-factor. The other sequence, LPC, gave rise to a very thick layer of adsorption. Almost 3 times thicker than HLT of PEO alone. It is even greater then the Stokes diameter of a PEO chain. The association of the PEO chains coating the latex particles with PEO/SNS complexes or clusters may gives multilayer of adsorption onto latex particles. A slight flocculation of the latex particles might also happen. But still this flocculation is not very

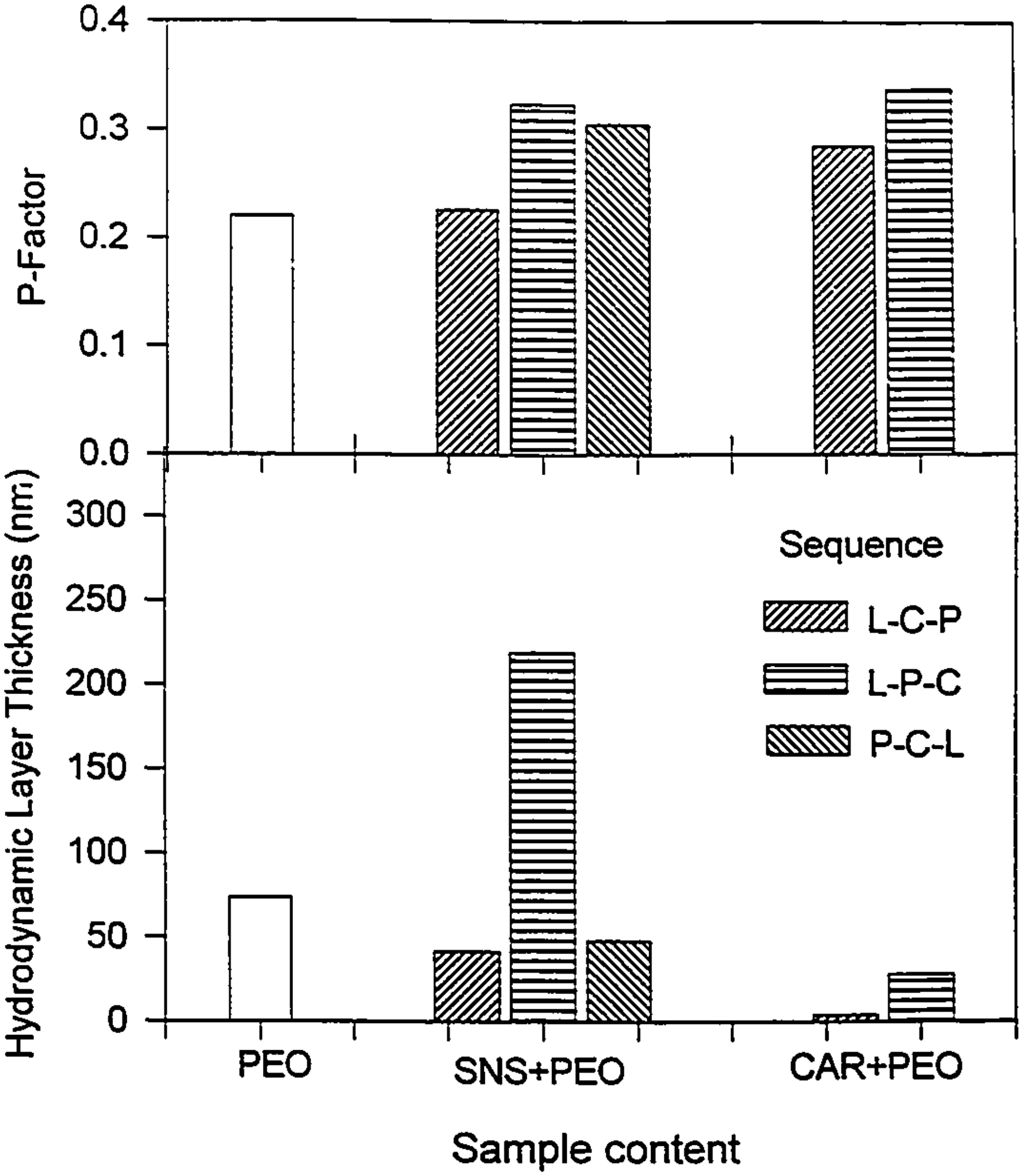

Figure 4: Effect of the sequence of addition on the hydrodynamic layer thickness. The hydrodynamic layer thickness and P-factor values are presented in the lower and upper graphs respectively. The values for PEO and with PEO/cofactors are presented. [PEO]=250 mg/L, [SNS]/[PEO]=5/1, [CAR]/[PEO]=10/1.

important because the P-factor is not very high.

Addition of CAR

Two sequences, LCP and LPC, have been investigated with CAR. In the first sequence, the HLT is negligible. A thicker HLT is obtained in the sequence LPC, but is still having a detrimental effect on PEO adsorption. This thicker apparent HLT can be due to particle-complex interactions. The PEO/CAR complexes seems to not adsorb onto latex but it takes time to desorb the initially adsorbed PEO chains. The P-factor is high for both of the sequences. The more important remark is that in both of the sequences, the adsorption of PEO chains is decreased when CAR is added.

3.2.2 Effect of the chemical ratio

The effect of varying the chemical ratio has been studied (figure 5). The chemical ratio is the relative amount of cofactor to PEO. This ratio is of primary importance in retention aid applications. The cofactor adsorbs onto PEO chains, increasing their entropy level. Such a modified PEO chain is more easily adsorbed onto a collector surface [1]. A minimum relative concentration (chemical ratio) is required for that to happen. From literature, the chemical ratio is often expressed as the number of cofactor molecules per PEO monomer unit [17-18]. The number of active sites, steric hindrance, and the molecular weight are also taken into account for phenolic resin compounds [13]. Having no precise characteristics about the cofactors, these quantitative characterisations were not possible.

Addition of SNS

SNS is the only cofactor that have been added in the second sequence, LPC. No significant increase is found from the ratio of 0 to 1. The critical concentration at which the adsorption happened is between the ratios of 1 and 5.

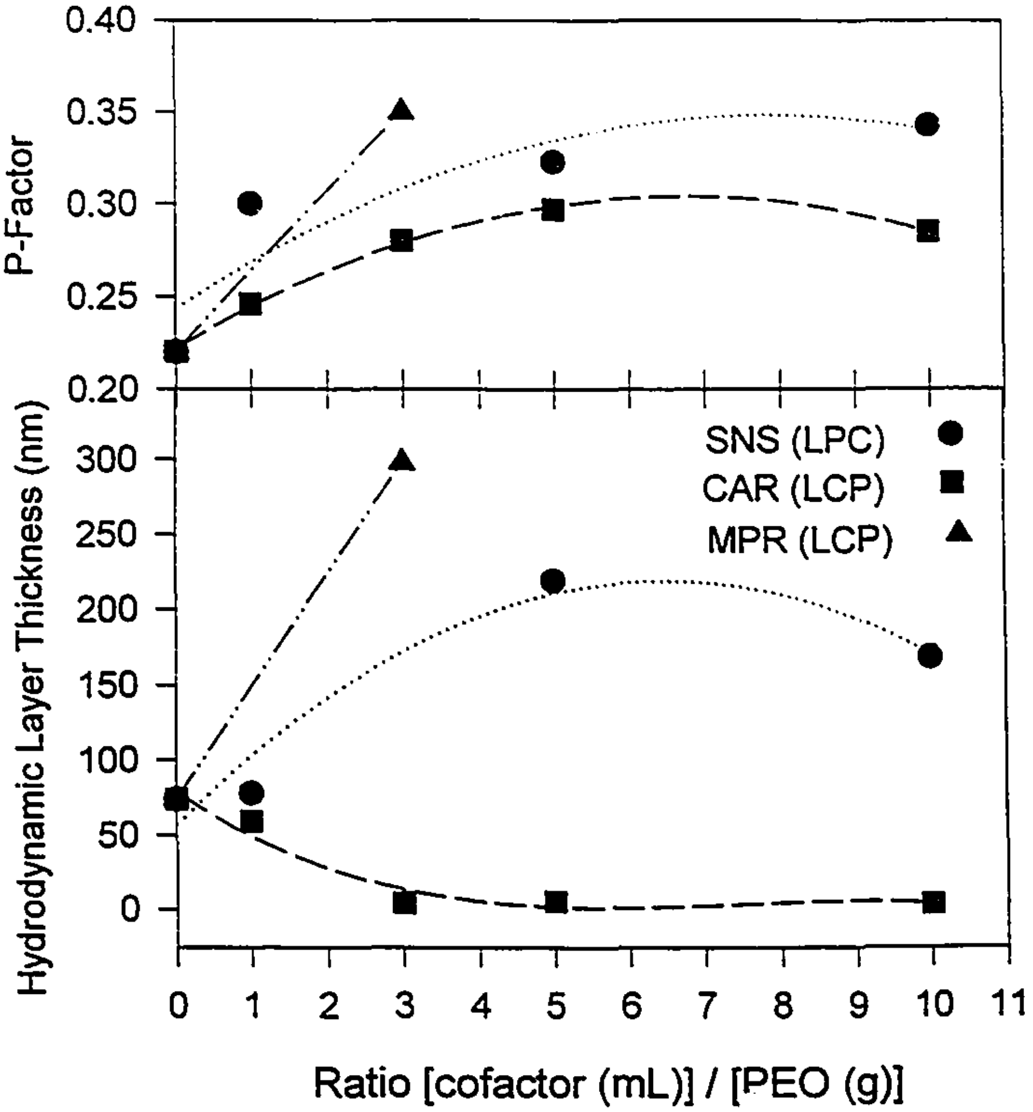

Figure 5: Effect of the chemical ratio on the hydrodynamic layer thickness. The hydrodynamic layer thickness and P-factor values are presented in the lower and upper graphs respectively. The values for PEO and PEO/cofactors are presented. [PEO]=250 mg/L. Lines are simply showing the tendencies.

The optimum for a maximum layer thickness is attained at a ratio of 5. A decrease in HLT from the ratio of 5 to 10 occurred. An explanation for this decrease, if significant, could be that PEO chains became coated by a greater quantity of SNS complexes or clusters. This may have the effect of a decrease in the adsorption efficiency. The P-factor had steadily increased with the ratio but without indication of an important flocculation of the latex particles.

Addition of CAR

Addition of CAR changed significantly the layer thickness even at a ratio of 1 to 1. No significant adsorption for ratios of 5 and 10 was found. The P-factor is only slightly increasing, indicating that no flocculation happened. The more CAR is added, the less affinity between PEO and latex particles.

Addition of MPR

This case have already been discussed in table II, but we can also see that MPR was more effective then the two other cofactors, even at a relatively low chemical ratio.

3.2.3 The effect of time on the hydrodynamic layer thickness

Once the polymers got adsorbed onto the collector surface, rearrangement of the molecules will start and usually leads to the flattening of the PEO chains onto the surface. This process can have major effects on the stability of a colloidal suspension if the layer thickness of the polymer becomes thinner than the distance over which the electrical double layer is effective. Another reason for a change in the layer thickness, with time, can happen when a competitive adsorption between two or more added chemicals occurs.

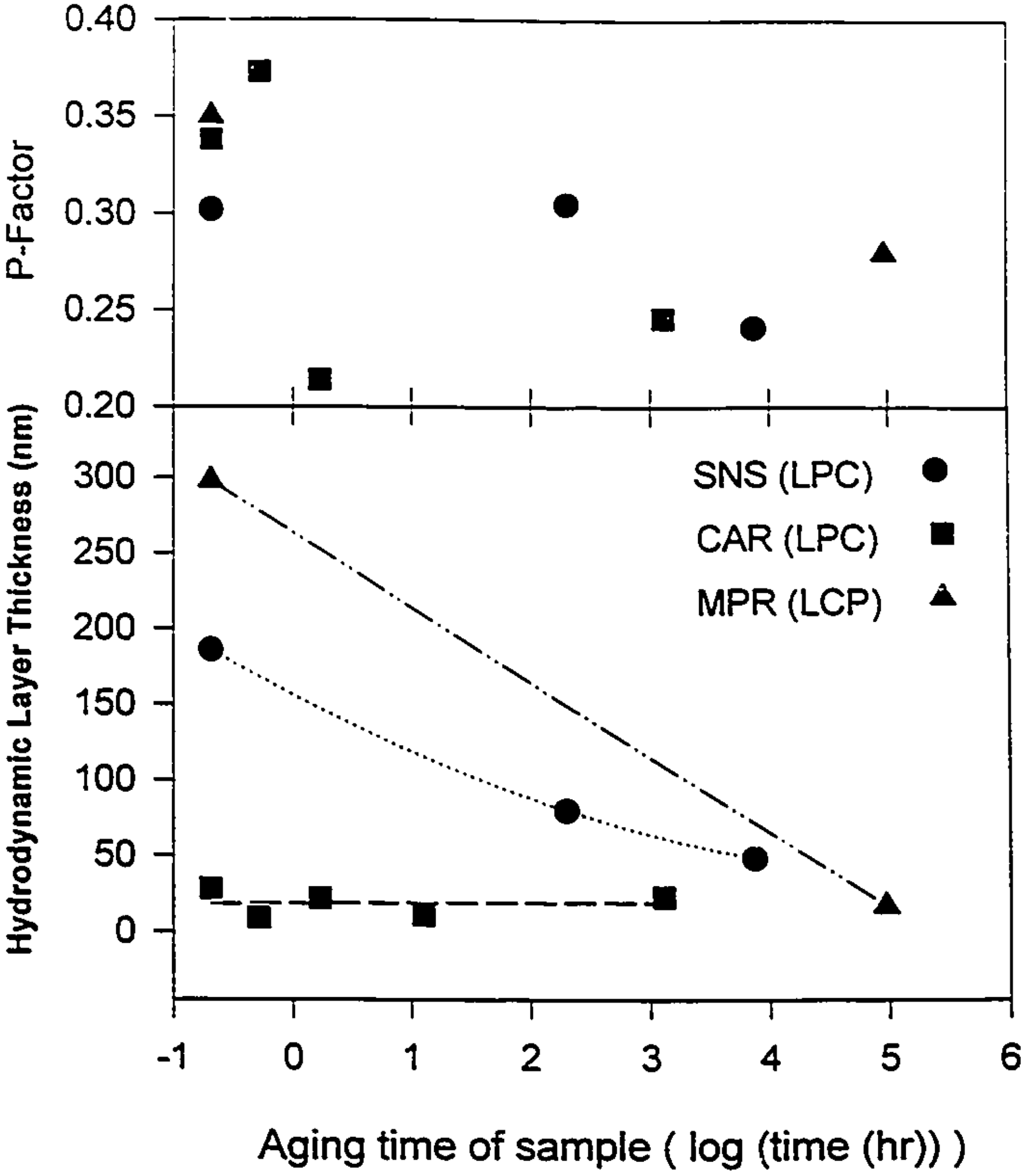

Figure 6: Effect of the sample aging time on the hydrodynamic layer thickness. The hydrodynamic layer thickness and P-factor values are presented in the lower and upper graphs respectively. The values for PEO and PEO/cofactors are presented. [PEO]=250 mg/L. [SNS]/[PEO] = [CAR]/[PEO] = 10/1. [MPR]/[PEO] = 3/1. Lines are simply showing the tendencies.

Addition of SNS

A four-fold decrease is found on the layer thickness within a period of 48 hours. The HLT at 48 hour sample aging is very similar to the HLT obtained in the sequence LCP and PCL shown in figure 4. This suggest that the system tends to a thermodynamic equilibrium which is readily attained when the cofactor is added prior to the PEO. The SNS is then possibly displacing the adsorbed PEO chains from the latex particles, decreasing the HLT. As a rule of thumb, the HLT (48 nm) measured onto a latex particles, scales with half of the polymer Stokes diameter (65 nm). A deflocculation of the coated particles, or desorption of PEO/SNS clusters, with time, can also explain the decrease in HLT value.

Addition of CAR

From the beginning, the HLT is low and keep this average over the time. The P-factor starts high, and has a tendency to decrease with time. That could be due to a slight, transient flocculation of the latex particles.

Addition of MPR

MPR has shown the greatest decrease in HLT with time, from 297 to 17 nm. A significant decrease in P-factor is also observed. A contraction of the PEO molecules might be the cause of the PEO flattening. In that case, electrostatic interactions may overcome the PEO/MPR layer thickness, and deflocculation of the slight flocculation (if present) occurred. Analogously to SNS, the final HLT of 17 nm scales with 32 nm for half the Stokes diameter of the PEO/SNS of figure 2.

4.0 CONCLUDING REMARKS

The effects of three cofactors (SNS, MPR, and CAR) on a polyethylene oxide of a molecular weight of $7\cdot10^6$ were studied with the use of Dynamic Light Scattering. The polymer free coil diameter was found to be in agreement with the literature [10]. Addition of each of the three cofactors to PEO solutions was found to create complexes. SNS did not change the apparent diameter significantly, but the CAR radically increased it. The PEO/CAR clusters are thought to be composed of CAR colloids. The MPR seems to decrease the size of the PEO chains.

The latex suspensions were also used to elucidate the behaviour of the cofactors. The HLT of PEO alone was in agreement with the literature [20]. In all experiments, CAR has shown deactivation of the latex particles for PEO. The SNS has been found very efficient in the sequence LPC, in increasing the PEO HLT. A thermodynamic equilibrium seems to take place at a HLT of about 40 nm. The mechanism by which the HLT is decreasing is thought to be due to a competitive adsorption between the cofactor and the PEO chains, or a rearrangement of the PEO/SNS complexes and clusters at the surface of the latex.

The MPR is the more efficient cofactor, in agreement with findings in literature. This is also the one from which the greatest difference in HLT with time was found. Because of the shrinking of PEO apparent diameter, rearrangement and flattening of the PEO chains is thought to be the cause of the decrease in HLT.

5.0 REFERENCES

1- van de Ven, T.G.M., Alince, B., *J. Pulp Paper Sci.*,(in press).

2- Polverari, M., van de Ven, T.G.M., *Colloids Surfaces*, 86, (1994), 209-228.

3- Berne, B.J., Pecora, *R., Dynamic light scattering, with applications to chemistry, biology & phisics*, John Wiley & Sons inc., (1976) ch.1-5,8.

4- Chu, B., *Laser Light Scattering*, Academic Press, New York (1974) ch.1-3, 6-8.

5- Schmitz, K.S., *Introduction to Dynamic Light Scattering by Macromolecules*, Academic Press, San Diego (1990) ch.1-5.

6- Brown, W., *Dynamic Light Scattering, the method and some applications*, Clarendon Press, Oxford (1993) ch.2, 4, 6.

7- Finsy, R., *Adv. Colloid Interface Sci.*, 52 (1994) 79-143.

8- Brandrup, J., Immergut, E.H., *Polymer Handbook*, John Wiley & Sons Inc.(1989) VII/3.

9- Napper, D.H. *Polymeric stabilization of colloidal dispersions*, Academic press inc., (1983) ch.1, 4.

10- Polverari, M., van de Ven, T.G.M., *J. Phys. Chem.*, (in press).

11- Fennel Evans, D., Wennerström, *H., The colloidal domain where physics, chemistry, biology, and technology meet*, VCH Publishers Inc., (1994) ch.7.

12- Schumacher, G.A., van de Ven, T.G.M., *Langmuir*, 7 (1991), 2060-2065.

13- Stack, K.R., Dunn, L.A., Roberts, N.K., *J. Wood Chem. Tech.*, 13, 2, (1993), 283-308.

14- Xiao, H., Pelton, R., Hamielec, A., *J. Polymer Sci.*, A, 33, (1995), 2605-2612.

15- Barker, G.E., Ranauto, H.J., *J. Am. Oil Chem. Soc.*, 32 (1955) 249-252.

16- Parrod, J., Kohler, A., *C.R. Acad. Sci.*, 246 (1958) 1046-1047.

17- Bailey, F.E., France, H.G., *J. Polym. Sci.*,49 (1961) 397-406.

18- Tadokoro, H., Yoshihara, T., Chatani, Y., Murahashi, S., *J. Polym. Sci.*, Part B, (Polym lett.), 2 (1964) 363-368.

19- Hild, G., Kohler, A., Parrod, J., *Bull. Soc. Chim. France*, 7 (1966) 2284-2288.

20- Couture, L., van de Ven, T.G.M., *Colloids Surfaces*, 54,(1991), 245-260.

CHAPTER III

STABILITY OF SUSPENSIONS OF FINES

1.0 INTRODUCTION

In chapter II, the three cofactors, carbamide (CAR), sodium naphthalene sulphonate (SNS), and modified phenolic resin (MPR) were found to associate with PEO. The results from the DLS experiments, combined with the knowledge of the properties of PEO solutions are certainly very relevant to elucidate the mechanism of flocculation of the PEO/cofactor systems. However, since the time frame of the adsorption and of the flocculation phenomena on model latex particles can be very different than on wood fibers, and cannot be directly applied to papermaking process. To link the model to the applications, flocculation kinetics experiments are performed on wood fines suspensions.

Flocculation kinetics provides a direct measurement of the efficiency of the collisions between the particles present in a reactor. The rate of collision is initially the same if the particle number and hydrodynamic conditions are kept constant. The parameter left is the collision efficiency, leading to flocculation, that can be changed by adding PEO and different cofactors (change in physicochemical properties). The objectives of this chapter are to quantify the flocculation behaviour of PEO with different cofactors, and to elucidate the mechanisms.

Segregation of fines from a thermomechanical pulp (TMP) is described followed by a description of the experimental montage and the basic theory of the photometric dispersion analyser (PDA). The specific adsorption of the cofactor is discussed. Stability graphs as a function of PEO concentration, sequence of addition and chemical ratio (cofactor/PEO) are presented.

2.0 EXPERIMENTAL

2.1 Materials

The polymer and cofactors were provided by E.QU.I.P. International Inc. The neutral polymer is a PEO of a weight-average molecular weight (M_w) of 7 millions with a polydispersity ranging between three and four. The cofactors are of three types: the first one contains sodium naphthalene sulphonate, and will subsequently be called SNS; the second one contains carbamide, CAR; and the third one is a modified phenol-formaldehyde resin, called MPR. The PEO was provided as a solid while the cofactors were commercial concentrated solutions (nearly 50% consistency).

Potassium chloride of analytical reagent grade was added to the dilution water to reproduce in laboratory the salt concentration of the white water found in a paper mill. To achieve this, the distilled-deionised water was salted with KCl, and the conductance was adjusted to 1.89 mS/cm, this gave a KCl concentration of 10^{-2} M.

The thermomechanical (TMP) pulp used was provided by Stone Consolidated Inc. Belgo division. The pulp was taken from the mixing chest and was at a consistency of 2.5%. The white water was collected from the Buffer chest, also called the dilution white water chest. The pulp was segregated and only the finer fraction (<200 mesh) was kept.

2.2 Segregation of the TMP pulp into two fractions: the fibers and the fines

The apparatus used to measure the stability of the wood fibers suspensions was based of the transmittance of the light passing through the flowing pulp suspension. A restriction on the path length of the light beam into the pulp suspension was to be taken into account. Because the wood fibers are relatively big, only the finer fiber fraction of the pulp suspension was then possible to flow through the chosen tubing (see section 2.4.2).

A segregation of the wood pulp fibers was then required. The first apparatus used was a Bauer McNett, well known to characterize the mechanical pulps. The fraction passing the 200 mesh filter was collected in 70 L containers. The standard procedure for fiber classification is described in the Tappi test method [1]. The limitation was on the quantity, only 3 grams of fines were collected at a time. The second option was to use an apparatus called Float Wash located in the mechanical pulp section, Paprican, Pointe-Claire, Québec. The Figure 1 depicts the apparatus.

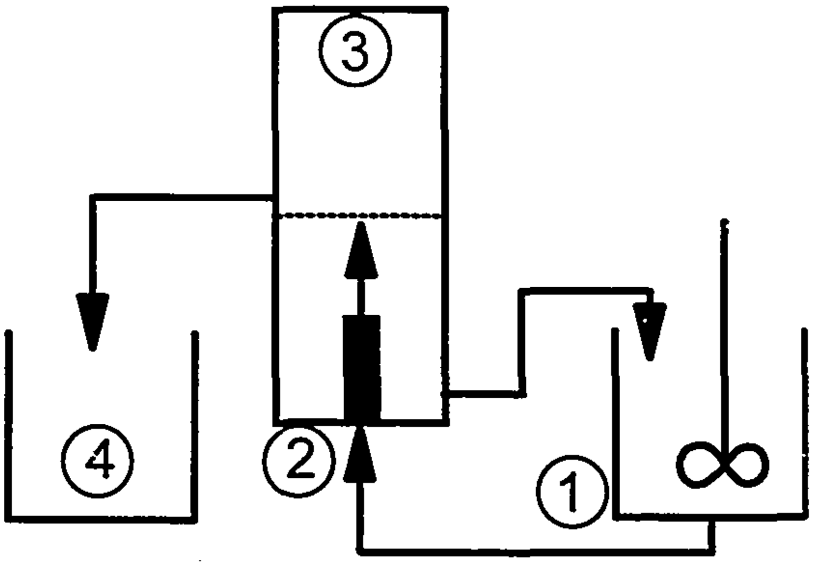

Figure 1: Schematic of the Float Wash apparatus composed of a mixing tank (1), the impinging cell (2), the suction cell (3), and the collector container (4). Fines are collected in (4) and fibers in (1).

The wood pulp (400 g. o.d.) was introduced in the mixing tank (1). Filtered tap water of a conductance of 297 µS/cm was added to the mixing tank for dilution to get the operating consistency. The pulp was circulated to the impinging cell (2). The jet of pulp impinged the filter separating this cell from the suction cell (3). The chosen filter was of 200 mesh in size (74 nm openings). What is not passing the filter is falling down the cell (2) and is recirculated to the mixing tank. A negative pressure was imposed to the cell (3) to collect the filtrate. The filtrate was directed to 70 L containers (4), and concentrated by gravity for a period of 24 hours. The supernatant was decanted to keep the bottom fraction (the fines) at a consistency of 0.6%. This fraction was kept to study the flocculation kinetics.

2.3 Solutions and suspensions preparation

Freshly distilled, deionized water was used to prepare aqueous fines suspensions. All the glassware used for chemicals make up and dilution was treated as in the chapter II. The reactor was washed with soap and rinsed with distilled deionised water between each chemical addition. PEO stock solutions were prepared at a concentration of 2 g/L prior to each experiment. The PEO solutions were stirred for 24 hours to completely dissolve the polymer and then put aside for another 24 hours without stirring before using it.

The cofactors stock solutions of 6 g/L were freshly prepared previously to each experiment from aqueous commercial samples.

A new fines suspension was always prepared between each chemical addition. The distilled deionised salted water was added followed by the required amount of the 0.6% fines pulp to get 0.05% consistency in the reactor. The PDA was set before the chemicals were added. Depending on the desired effect, the cofactor or the PEO was added prior to the other. Fifteen seconds were separating the addition time of each chemical to ensure good mixing. The concentration of the chemicals (PEO or cofactors) is expressed in ppm (10^{-6}g of chemical/g of fines).

2.4 Instrumentation and analysis

2.4.1 Specific adsorption of cofactors onto wood fines

An experiment was performed to elucidate wether or not the cofactors are adsorbing onto the wood fines. Such knowledge is critical for interpretation of the results. For a cofactor which is adsorbing onto the fines particles, a very different behaviour can be found if it is added before or after the polymer. A cofactor adsorbing onto fines will initially cover the fines surface and will be present in the bulk solution only if excess is added. However a cofactor which do not adsorb onto the fines surface will remain in the bulk solution. These differences might influence the mechanism of flocculation.

Since two of the cofactors of interest contain phenyl groups absorbing high on the UV range (280 nm), a UV-spectrophotometer is the instrument of choice to measure the specific adsorption (S.A.) of the cofactors. A UV-visible spectrophotometer Varian Cary 1E equipped with quartz cuvettes (pathlength of 1 cm) was therefore selected.

Only the supernatant from the pulp suspension was to be analysed by spectroscopy. The samples had to be prepared to meet a chosen relative weight of cofactor to the weight of fines. Two constraints complicated the experiment: the required relatively high cofactor concentration to be detected by the spectrophotometer and the difficulty to manipulate a medium consistency wood fines pulp. The cofactors were added to suspensions at concentrations of 100 and 200 ppm. A Sorvall RC-5B, refrigerated superspeed centrifuge, from DuPont Instruments was used to get the desired pulp consistency. The original fines suspension (0.6% consistency) was salted to 1.89 mS/cm and then thicken to 3% for the 200 ppm experiment and to 4.7 % for the 100 ppm one. A set of sample cells was prepared with the fines pulp, in which the cofactors were added. The samples were stirred and centrifuged at 12 000 RPM for 20 minutes. The supernatant was collected and analysed to determine the residual cofactor in the bulk solution. Blank samples, in which no cofactor were added, were also made following the exact same procedure to make the baseline for concentration determination.

2.4.2 Stability of suspensions of fines

When a suspension becomes unstable, the particle size is increasing or decreasing. A photometric dispersion analyser (PDA-2000), from Rank Brothers LTD, was used to measure the flocculation rate constants by quantifying the change in the relative particle size [2-5]. The details of the PDA apparatus are presented in Figure 2. It consist of a reactor (1) of a capacity of 1 L. The inside diameter of the reactor is 10 cm. The suspension was stirred at 100 RPM by a RPM-display stirrer (2) with a single blade paddle of 8x3 cm. The suspension was flowing through a 1.6 mm id. Tygon tubing (3). The tube length between the reactor and the light probe (6) was 37 cm. Such a small tubing diameter is allowing us to assume the laminar flow theory at the flowrate used [3]. The suspension was flowed through closed circuit by a micropump (4), at 50 mL/min with the help of a flowmeter (5). The light probe (7) is constituted of a narrow beam of light passing transversely through the tube [2]. The source light is a light-emitting diode of 0.1 mm wide with a wavelength of 820 nm.

The basic theory is resumed here. The intensity, I, of the light transmitted through a particle suspension is [2],

$$I = I_o \exp(-\boldsymbol{n} K l) \qquad (1)$$

where I_o is the emitted light intensity, $\boldsymbol{n}$ is the particle concentration, K is the average

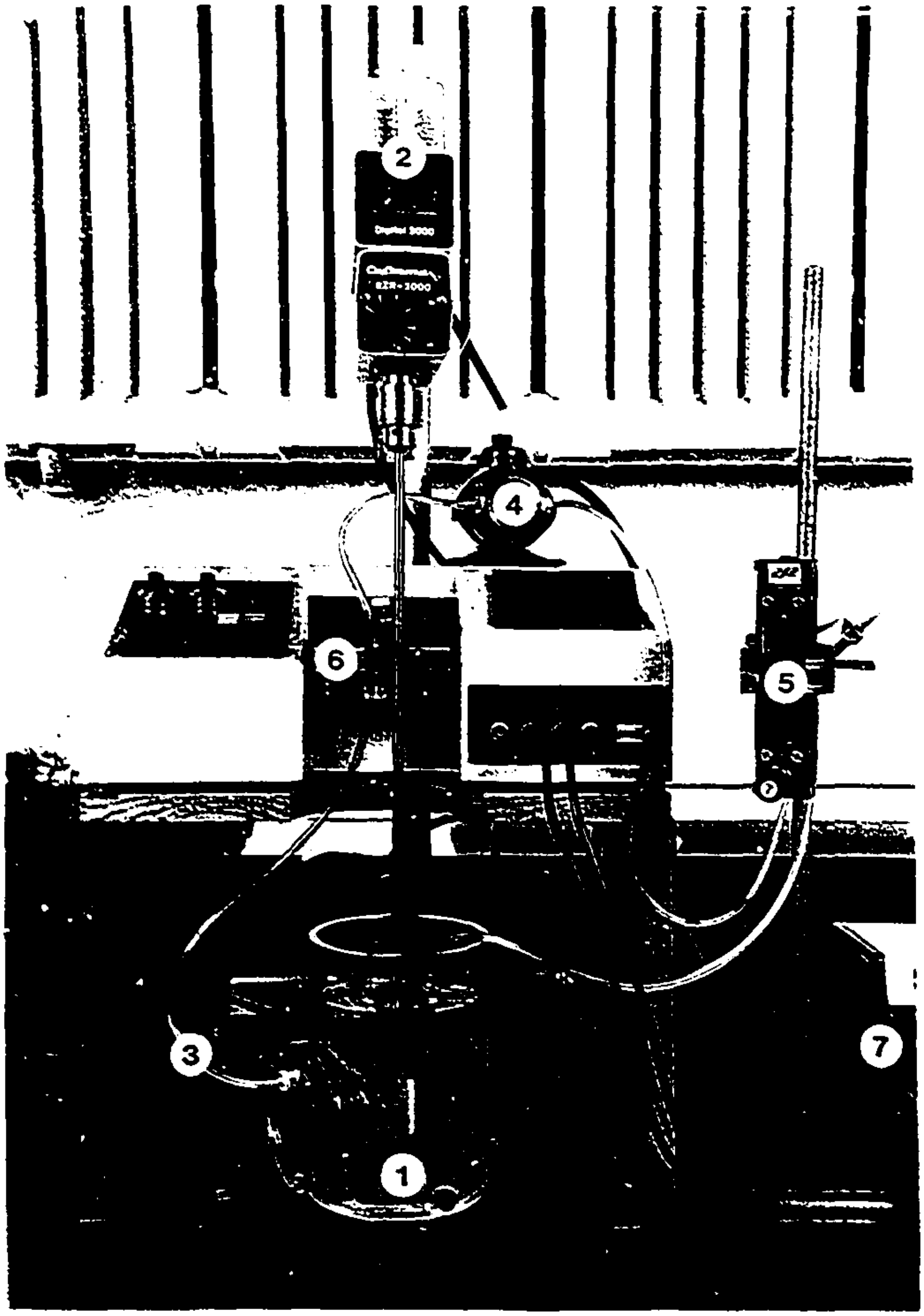

Figure 2: Flocculation testing montage comprising the 1L reactor (1), the stirrer (2), the 1.6 mm id. tubing (3), the gear pump (4), the flowmeter (5), the transmittance cell (6), and the chart recorder (7).

scattering cross-section of the particles and, l, is the optical path length. One should be aware that the following development is valid only if a small fraction of the light is scattered, so that $I/I_0 \approx 1$ and nKl « 1. The intensity fluctuations arise from random variations in the number of particles in the beam, n_p:

$$n_p = n l A \qquad (2)$$

where A is the beam cross-section area. The light intensities are measured as voltages. Since the RMS value of the number fluctuations is $n_p^{1/2}$ (assuming Poisson distribution,) the RMS voltage, V_{rms}, is,

$$V_{rms} = V_o n_p^{1/2} \frac{K}{A} \qquad (3)$$

Two of the variables, n_p and K, change when flocculation happen. Keeping low the particles concentration in the reactor minimises the variation in n_p value. The transmittance is simultaneously monitored as V_{dc}. The transmitted intensity should then not vary more than a few percent during the flocculation process. The scattering cross-section, K, can be described as,

$$K = 2\pi a^2 \qquad (4)$$

and is proportional to the square of the particles radius for the ideal case of spherical ones. To minimise the effect of the variation in particle concentration, I or V_{dc}, the change in RMS of the intensity, V_{rms}, was combined with the former one to give a ratio R (= V_{rms}/V_{dc}). The rate of change of this ratio R, is monitored with a chart recorder and is taken as the rate of flocculation constant, k_i, that can be compared from one experiment to another.

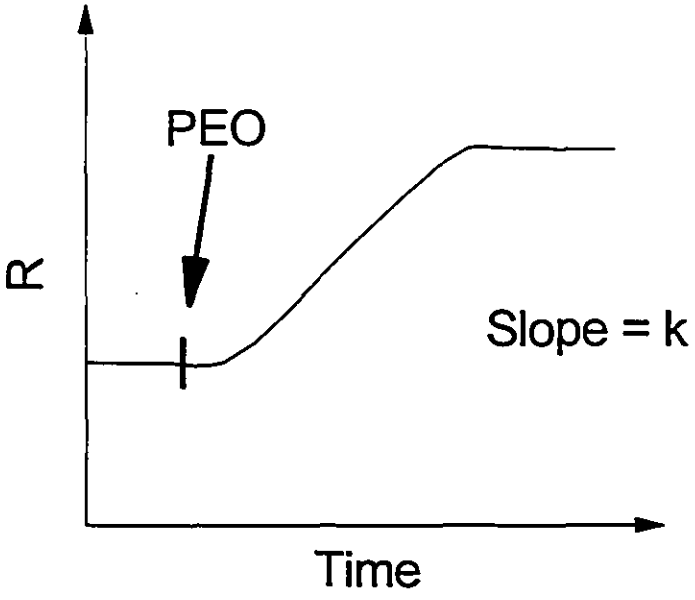

Figure 3: Schematic of the recorded response on the chart recorder. R is the ratio V_{rms}/V_{dc} as a function of time. The slope represents the rate of change of the size of the particles. The flocculation occurs shortly after the polymer is added.

The stability ratio, W_i, is defined as the ratio of the fastest flocculation rate constant, k_{fast}, over the given flocculation rate constant of one experiment, k_i:

$$W_i = \frac{k_{fast}}{k_i} \tag{5}$$

Two limiting cases are of interest, the logarithm of a stable suspension (when the chemicals do not perturb the system), is equal to infinity, and the logarithm of the less stable suspension is equal to zero.

3.0 RESULTS AND DISCUSSION

The Figures 4, 7 and 10 show the results obtained on the destabilisation of suspensions of fines by the aid of the PEO-cofactor dual retention-aid system, while schematics representing the proposed mechanisms are illustrated with Figures 5, 8 and 9. The addition of PEO alone (without adding any cofactor,) the effect of the sequence of addition of the cofactor and the polymer, as well as the variation of the chemical ratio (cofactor/PEO) are discussed in terms of fines flocculation.

3.1 Relative concentrations

It is useful to have an idea of the relative amount of chemicals to the wood quantity in the reactor. From rough estimations, it is possible to know if a chemical, PEO or cofactor, is fully coating the fines. It should be mentioned here that this can happen only if a given chemical adsorbs onto the fines.

A number average Stokes diameter of 19 μm for the fines, was found using a centrifugal particle sizer, the BI-DPC from Brookhaven Instruments Co. The fines density was assumed to be 1.36 g/cc. A specific surface was calculated assuming the fines to be spherical. The result is 0.223 m^2/g of o.d. fines. If the same method to approximate the specific surface of clay particles is used, a difference of 10% is made if compared to the value determined by nitrogen adsorption [6]. The reactor contains 1L of a 0.05% consistency fines suspension for a total of 0.5 g o.d. This gives a surface of 0.111 m^2. As a rule of thumb, the specific adsorption for the cofactors and the PEO are 0.1 and 1 mg/m^2 respectively. These quantities are in mg solids, and the consistency of the cofactors in the commercial solutions are roughly 50%. From all these assumptions and approximations, an

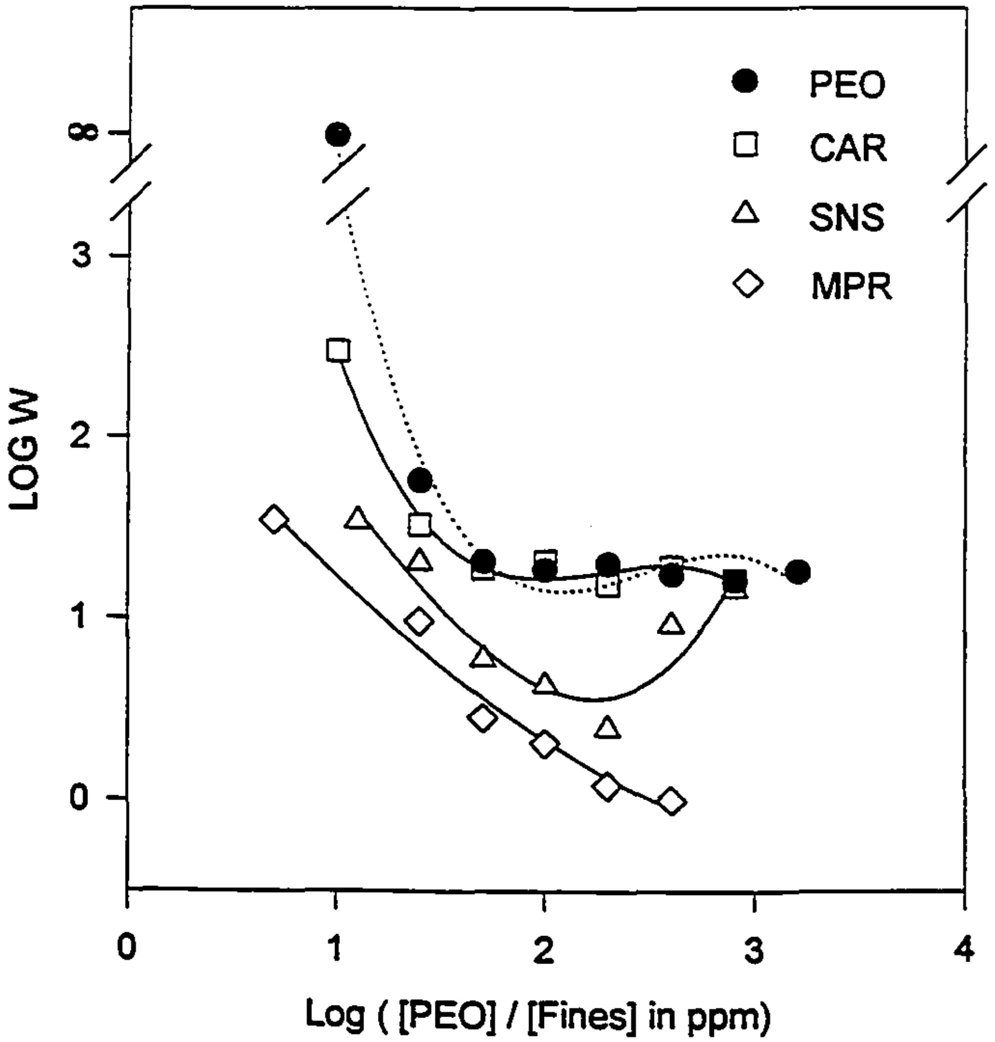

Figure 4: Stability graph of suspensions of fines in the sequence of addition fines-cofactor-PEO (FCP). Ratio [cofactor]/[PEO] = 3/1, [KCl] = 10^{-2}M.

The fines particles are thought to be dissimilar in three aspects: in size, shape, and in surface properties. The last one is causing the heteroflocculation behaviour and is likely to be due to the differences in lignin content of the fines structure. Several studies confirmed that lignin content in fines may vary with the particle size or the type of fines [9-10]. The present case can be modelled with two types of fines: one being completely covered with lignin, type A, and the other consisting of pure cellulose, type B. PEO is known to adsorb onto hydrophobic particles [11-12], but not onto hydrophilic cellulosic fibers. The number of collisions, f, leading to coagulation per unit volume per unit time is,

$$f = \alpha\, k_{AB}\, n_A\, n_B \tag{6}$$

where n is the particle concentration, k_{AB} is the collision rate constant and the subscripts hold for the fines types A and B respectively. The particle concentration being the same from one experiment to the other, a constant stability ratio is obtained. The fastest flocculation rate is attained at full coverage of type A fines, and steric stabilisation will never occur [8]. Such a model involving two types of fines can explain the behaviour of the PEO plot shown in Figure 4. The type A, the hydrophobic one, is already fully coated at a PEO concentration of 50 ppm (Fig. 5 (a)). The lignin-coated particles are thought to act as a cofactor [8, 13]. Once PEO is adsorbed onto the surface, the degree of freedom of PEO chains is reduced, rending possible their adsorption onto the type B. Bridging of the two particle types is then possible.

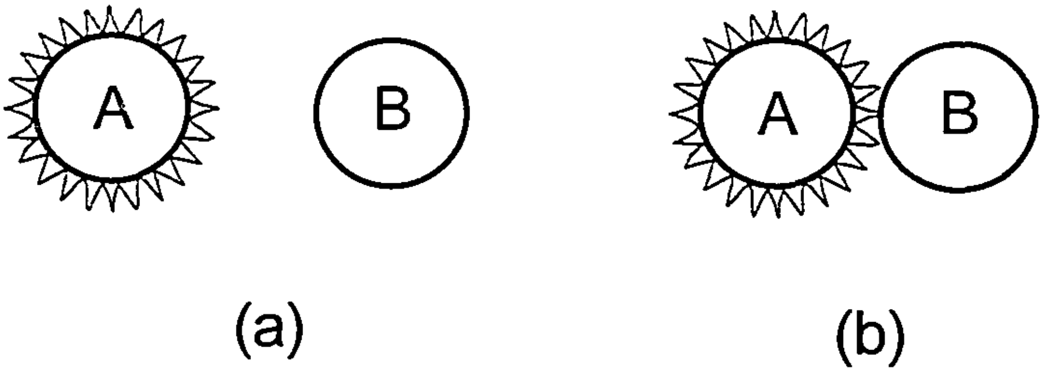

Figure 5: Heteroflocculation of fines by PEO. (a) Type A fines becomes fully coated at 50 ppm of PEO, but the type B remains uncoated at any concentration. During adsorption, the PEO chains adopt a modified configuration and undergo an entropy gain. The type A fines is acting as a cofactor. (b) The adsorbed PEO onto type A can adsorb on the type B by association-induced polymer adsorption. The required loss in entropy for adsorption of the modified PEO chains onto the type B is less and bridging occurs.

3.3 Specific adsorption of SNS and MPR

The calibration curves for SNS and MPR were established. The values of 150 and 26.9 L/g were found as the coefficients for the absorbency by SNS and MPR respectively. The CAR was not detectable by the UV-spectrophotometer and then not tested.

The results from the spectrophotometer revealed specific adsorptions of the cofactors on the wood fines of 68.2 and 7.7 µg/g o.d. for SNS and MPR respectively. The SNS does adsorb onto the fines but the value for the MPR was not significant and then giving no proof of its adsorption onto wood fines.

3.4 Effect of the sequence of addition of the chemicals on the stability of suspension of fines

The order of addition of the chemicals can make a difference in the flocculation mechanism. That happened for SNS and MPR. Flocculation process is usually diffusion controlled [5, 14]. Even in sheared suspensions, perikinetic (diffusion) adsorption is more important for relatively smal particles or molecules like PEO and cofactors. Because the suspension is continuously stirred, fines-fines collisions will be more frequent than PEO-fines or cofactor-fines collisions. Orthokinetic flocculation can be important for relatively big particles like fines in sheared suspensions. Also depending on the nature of the cofactor, the collision efficiency, α, of the cofactor-fines interactions will be different from zero, only if it can adsorb onto the fines.

Two different sequences of addition are presented in figures 4 and 7, fines-cofactor-polymer (FCP) and fines-polymer-cofactor (FPC) respectively. The former one was made by preparing the fines suspension, F. Thereafter, the cofactor, C, was added to the suspension prior to the polymer, P. In the second sequence (Fig. 7), the cofactor was added last.

It should be noted that the baseline from which the relative particle size is compared (single or aggregated particles) was different for the two cases. In the sequence FCP, no flocculation was found prior to the addition of PEO, and that for any cofactor concentration (Fig. 3). The baseline was the one of the originally stable fines suspension. In the second sequence, FPC, flocculation occurred after the addition of the PEO. The baseline was then the fines suspension flocculated to a certain degree (Fig. 6). Therefore, the flocculation rate (if occurred) was measured on the second sharp increase in relative particle size. The relative efficiency of one sequence to the other can not be compared.

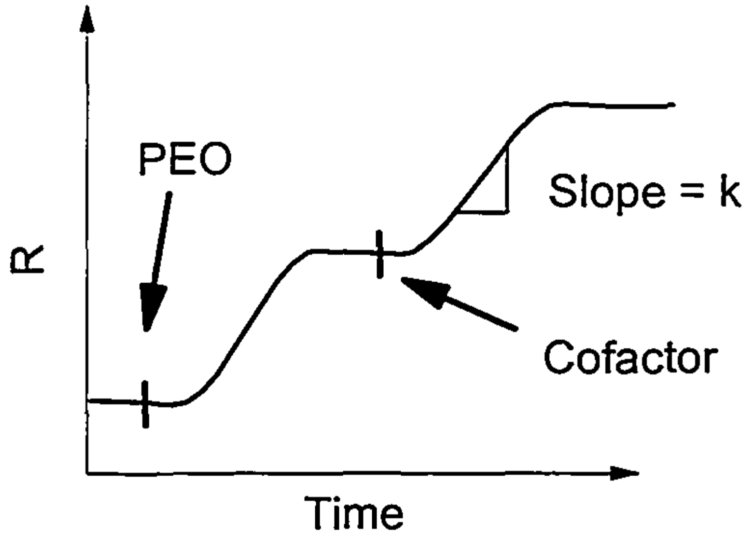

Figure 6: Rate of change of the ratio R in the sequence fines-PEO-cofactor. The first flocculation occurs after the addition of PEO. A subsequent flocculation occurs when the cofactor is added. The flocculation rate constant is calculated from the second increase in relative particle size.

Addition of CAR

In the sequence FCP (Fig. 4), the results are following the same trend as when PEO was added alone. This is an evidence that the addition of the CAR prior to PEO neither change the surface properties of the fines nor enhance the PEO adsorption. The formation of PEO/CAR complexes (proposed in chapter II,) did not influence the flocculation process. In the other sequence (FPC), complete stability was observed (Fig. 7). Referring to the Figure 6, no flocculation was found after the addition of the cofactor. The same conclusion as in the former sequence is brought. The two CAR plots are showing the same trend.

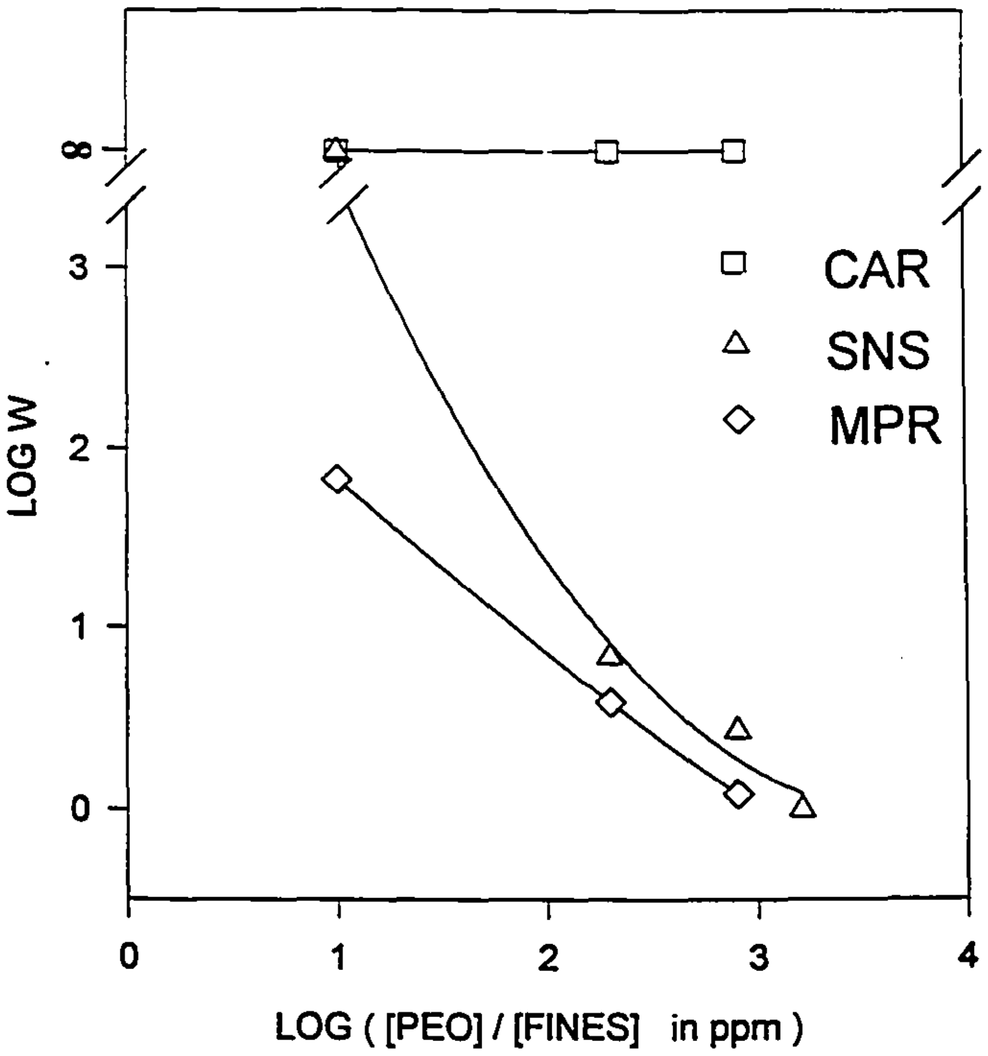

Figure 7: Stability graph of suspensions of fines in the fines-PEO-cofactor (FPC) sequence of addition. Chemical ratio = 3/1, [KCl] = 10^{-2} M.

Addition of SNS

From the SNS plot in Figure 4, a suspension of fines is already destabilised at a PEO concentration of 12.5 ppm. An optimum in the flocculation rate was observed at a PEO concentration of 200 ppm. On the other hand, in Figure 7, the SNS was added after the PEO, and the more PEO was added, the faster was the flocculation in the range of concentration studied. No optimum was found.

The former behaviour of SNS in Figure 4 is typical of homoflocculation. It happens when all the particles are alike in surface properties. An optimum in the flocculation rate is found at about half coverage of the particles by the polymer [8, 15]. At lower concentration, the electrostatic repulsion decreases the collision efficiency while the steric repulsion yields the same effect at higher concentration. The SNS does adsorb onto fines surface, and full coverage by the cofactor is to occur at about 12 ppm of PEO in Figure 4 and 7 (calculated from S.A. of 68 μg/g of fines). This has the effect of making all the particles alike. When the PEO is added to a suspension of SNS-coated fines, the PEO chains adsorb onto all types of particles. Because full coverage of the fines particles occurs at very low SNS concentration, one cannot distinguish between the two following possibilities: I) the PEO chains bridge SNS-coated particles or ii) PEO/SNS complexes bridge bare particles.

In the sequence FPC from the Figure 7, the situation is different. The PEO being introduced prior to the cofactor, the flocculation rate constant is taken from an already heteroflocculated pulp suspension (figure 8 (a)). At any PEO concentration above 50 ppm, when the cofactor is added, the PEO is already adsorbed onto the fines and is also present in the bulk solution. At approximately 50 ppm of PEO, heteroflocs are present and subsequently added SNS covers the agregated particles to increase the bondstrength and give bigger flocs. The SNS could decrease the detachment rate constant [16]. Thus, the floc size can get bigger in the same hydrodynamic conditions.

The following mechanisms are proposed. In the sequence FCP at PEO concentrations lower than 50 ppm, bridging of SNS-coated particles might happen. At all other PEO concentrations, a combination of the former mechanism and bridging of bare and SNS-coated fines particles by PEO/SNS complexes may happen.

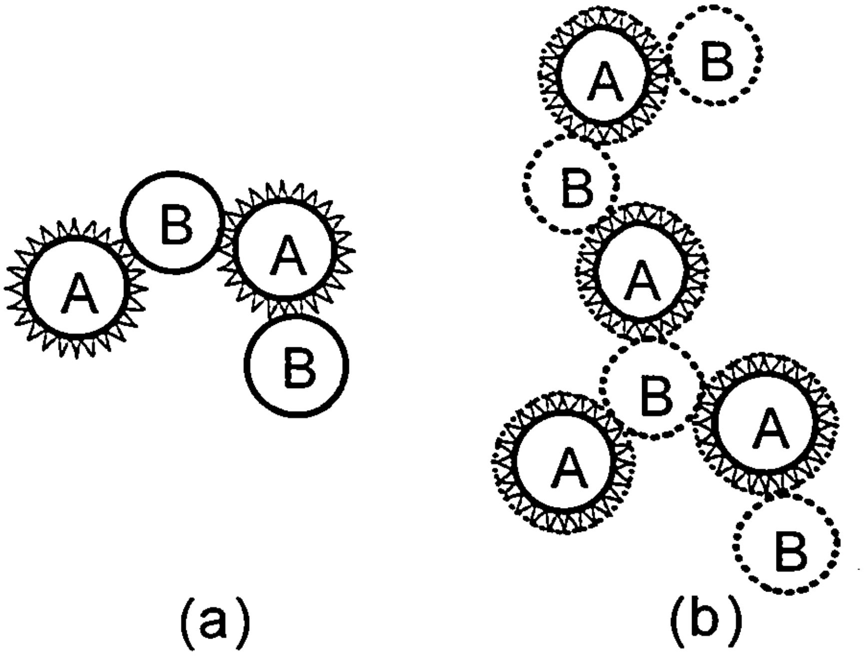

Figure 8: Sequence FPC. Increase in bondstrength by SNS at low PEO concentration (around 50 ppm). (a) Heteroflocculation by PEO alone. (b) SNS (dotted lines) can adsorb onto all types of particles, coating the bare and PEO-coated surfaces. The time required to detach a particle from a floc has increased due to the presence of SNS but the hydrodynamic conditions being the same, the time required for a particle to deposit onto a floc remains the same. Consequently, the floc size has increased.

Addition of MPR

The same flocculation behaviour is observed irrespectively of the sequence of addition when the modified phenolic resin (MPR) is used as cofactor (Fig. 4 and 7). The more concentrated the chemicals are, the higher the flocculation rate. As explained for SNS, the absolute values cannot be compared from the FCP to the FPC plots.

Lets start by the MPR plot in Figure 7. The same trend as SNS is found but with a much higher efficiency at low concentration. The same mechanism as for SNS, regarding the possible decrease in the detachment rate constant is proposed. The difference is that in the sequence FPC, at PEO concentration lower than 50 ppm, the cofactor adsorbs onto PEO-coated (type A) particles only (Fig. 9). The MPR modified PEO-coated particles then become more sticky which allow further flocculation to occur. At high concentration, formation of PEO/MPR complexes is probably becoming the most abundant species and then association-induced polymer bridging occurs.

In the figure 4, where the MPR was added prior to PEO, no deposition of the cofactor onto the fines is to occur since no significant specific adsorption was found by spectroscopy. The cofactor is free in the bulk solution instead of coating the fines as SNS does. When the polymer is added to the suspension of fines and MPR (not adsorbing on each other) two cases might happen: the cofactor molecules can adsorb onto the PEO molecules, or the PEO molecules can adsorb onto the fines. The adsorption time for each of these mechanisms can be estimated from the Smoluchowski theory. Assuming that the particle concentration, n_1, and the rate constant, k_{12}, remain constant, the time, t_{ads} required to adsorb a fraction, f, of the added polymer onto the fines or the cofactor molecules is [5]:

$$t_{att} = \frac{-\ln(1-f)}{k_{12}\, n_1} \tag{7}$$

where indices 1 and 2 represent the PEO, and fines or cofactor respectively.

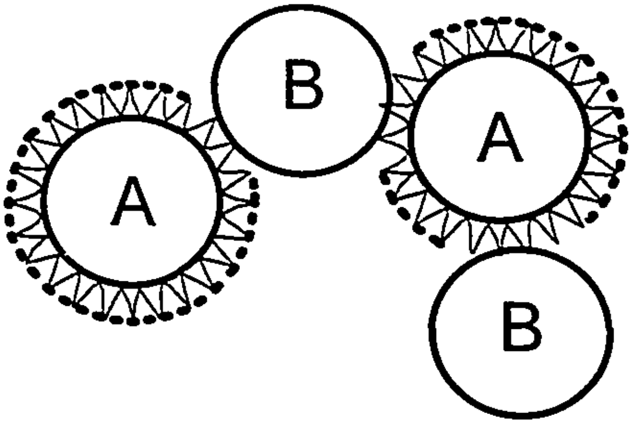

Figure 9: Adsorption of the MPR (dotted lines) onto a heterofloc created by adding PEO prior to the MPR. MPR adsorb only onto PEO chains.

As mentioned previously, adsorption and flocculation can occur via perikinetic or orthokinetic processes, depending on the size of the particles or molecules. The flocculation rate constant for *perikinetic* adsorption is:

$$k_{12} = \left(\frac{2kT}{3\mu}\right) \frac{(a_1+a_2)^2}{a_1 a_2} \tag{8}$$

where kT is the thermal energy, μ is the viscosity, and a is the particle or molecule radius. The flocculation rate constant for *orthokinetic* adsorption is:

$$k_{12} = \frac{4}{3} G (a_1 + a_2)^3 \tag{9}$$

where G is the shear rate in s^{-1}. One can determine the relative importance between the perikinetic and orthokinetic processes for a set of two particles by dividing t_{peri}/t_{orth}. t_{peri} is t_{att} after substitution of equation (8) into it. Equation (9) has been substituted in (7) to obtain t_{orth}. The resulting equation for water at 25°C, and a shear rate of $1.4 \cdot 10^3$ s^{-1} is:

$$\frac{t_{peri}}{t_{orth}} = 584 \cdot 10^{18}\ a_1 a_2 (a_1 + a_2) \tag{10}$$

The Stokes radius of PEO is about 50 nm (a_1) and the cofactor radius is taken as 7.5 nm (a_2) as found in section 3.1 of chapter II. A ratio of $12 \cdot 10^{-3}$ is calculated indicating a diffusion-controlled process. When a_2 is taken as the radius of the fines (9.5 µm), we obtain $2.6 \cdot 10^3$ indicating a shear-induced transport process. The relative importance of the perikinetic to the orthokinetic processes can be evaluated by deriving a similar equation as number (10): the PEO-cofactor interaction being at the numerator and the PEO-fines being at the denominator. The PEO-cofactor interaction is of 4 orders of magnitudes longer, suggesting that the PEO is adsorbing onto the fines first and then the cofactor molecules are adsorbing onto the PEO-coated fines. Equation (10) requires the hypothesis that the total surface area of the cofactor (spherical shape assumed) is equal to the total surface area of the fines.

That could explain the similar shape of the plots in Figures 4 and 7 where adding the cofactor before or after the PEO leads to the same mechanism.

3.5 Effect of the chemical ratio

This study was performed in the sequence FCP for a constant PEO concentration (200 ppm) where the half coverage is assumed from the previous SNS discussion. The results are presented in Figure 10.

Addition of CAR

Again, the addition of CAR was not successful at any chemical ratio. The same stability as when PEO is added alone at 200 ppm was measured.

Addition of SNS

The higher the SNS concentration, the greater the flocculation rate. Full coverage of fines occurs at about the lowest ratio measured. Consequently, SNS was present in the bulk solution for most of the range studied, and the formation of PEO/SNS complexes is likely to happen. At very high chemical ratio, PEO chains should be fully coated by SNS and steric repulsion between SNS-coated PEO chains and SNS-coated fines is expected to restrict the flocculation. In the range of ratio studied, it is possible that the SNS concentration was not high enough to significantly cover the PEO chains before they collide with the fines. Then the optimum is probably located at a higher chemical ratio where steric repulsion starts to inhibit the flocculation process.

Addition of MPR

An optimum is found at a chemical ratio of 10 to 1. At the chemical ratio used in papermaking applications (between 1 and 10,) the MPR was more efficient than SNS. The MPR molecules stay in bulk solution, never acting as a dispersant. The fact that a suspension is more stable when a relatively high chemical ratio (100 and 1000) is applied can be explained by the occupation of all the active sites on PEO by the MPR molecules [17].

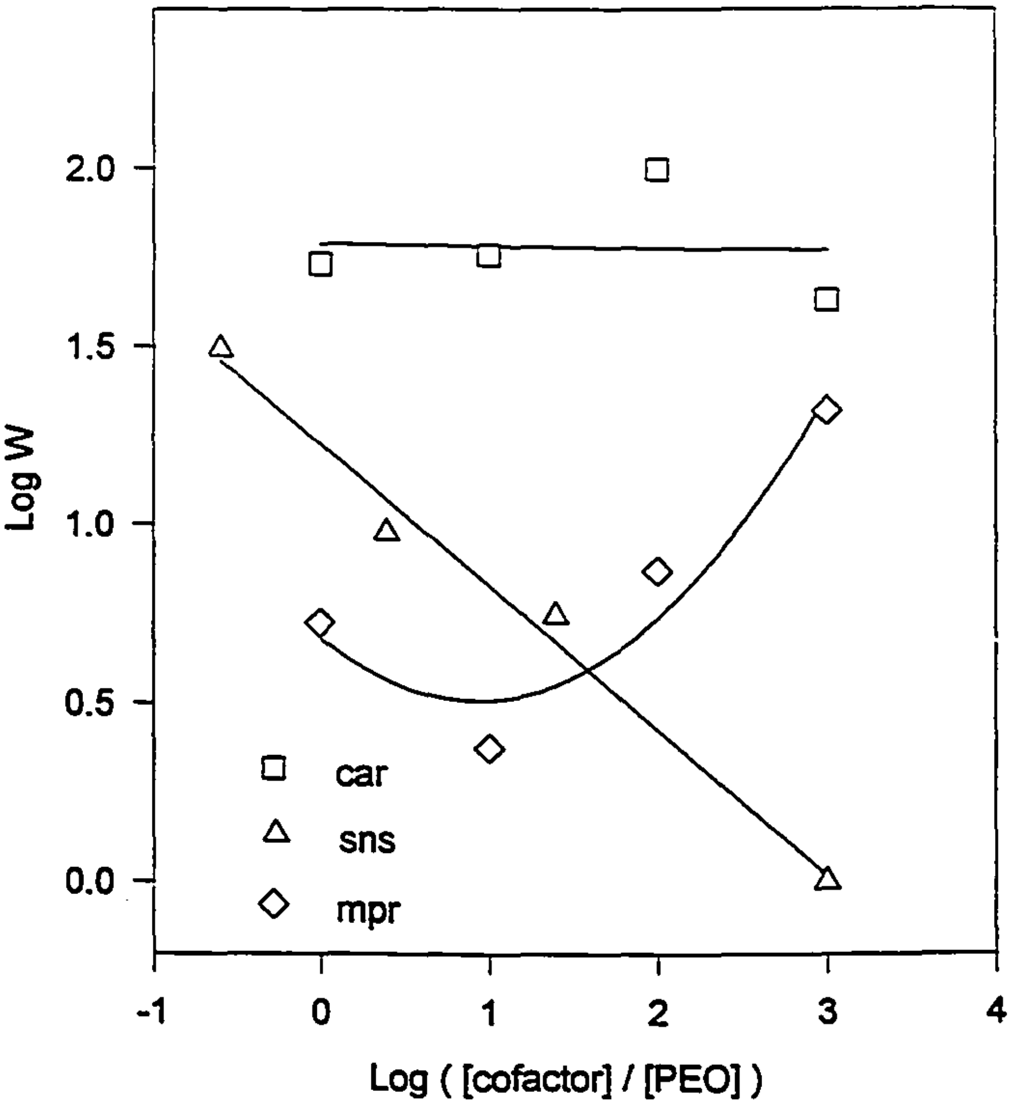

Figure 10: Stability graph of fines suspensions in the fines-cofactor-PEO (FCP) sequence of addition. [PEO] = 200 ppm. [KCl] = 10^{-2} M.

The PEO molecules are probably having more collisions with the fines than MPR molecules. However, since the successful collisions only happen with the fines of type A, then PEO-MPR collisions have more time to occur. This might explain the lower (relatively to SNS) chemical ratio needed for the optimum to occur. The MPR molecules anchored onto the PEO chains may increase the electrostatic repulsion between bare fines and MPR-coated polymers, leading to stable suspension.

4.0 CONCLUDING REMARKS

Flocculation kinetics studies were performed on suspensions of wood fines. A polyethylene oxide (PEO, M_w of 7 millions) was used in combination with three different cofactors: SNS, CAR, and MPR.

The specific adsorption of the cofactors onto the fines was also studied. SNS was found to adsorb (68.2 µg/g o.d. of fines) onto the fines whereas MPR did not. The stability of the fines suspension was measured with a photometric dispersion analyser. The technique, based on the measurement of the variations of the transmitted light, quantifies the flocculation rate constant. The flocculation behaviour of fines with PEO alone is fully supported by the mechanism of asymmetric heteroflocculation involving two different types of fines. We therefore propose the fines fraction to be made of two components: lignin coated fines (on which PEO asdsorbs), and cellulose fines (no PEO adsorption).

CAR was found to create complexes with PEO in chapter II. Hydrogen bounding is thought to be operative between a PEO and a CAR molecule. However this seems to be insufficient to flocculate a pulp suspension, and other cofactors containing phenolic groups like SNS and MPR are much more efficient.

SNS can adsorb onto all the fines making them alike. Adding the PEO after SNS gave homoflocculation, where the half coverage was assumed to happen at the fastest flocculation rate. The specific surface of fines, calculated by PEO adsorption was found to be 0.223 m^2/g. When the PEO was added prior to the SNS, a decrease in the detachment rate constant is likely to happen. The particles are thought to become more sticky with the addition of the cofactors. The same mechanism occured for MPR when added after the PEO. In the other addition sequence (FCP), no difference was found in the mechanism of flocculation when MPR is used. Because the MPR does not adsorb onto the fines, and that the flocculation process is diffusion controlled (PEO-cofactor interaction is slower than PEO-fines), heteroflocculation of the fines is likely to happen before the bondstrength is increased by the MPR.

The PEO alone can certainly flocculate a suspension of fines. However adding cofactors such as SNS and MPR significantly decrease the stability ratio by a few orders of magnitude.

5.0 REFERENCES

1- TAPPI test methods, *T1-T1209*, TAPPI Press (1992) T233 cm-82.

2- Gregory, J., Nelson, D.W., *A new optical method for flocculation monitoring*, In Solid-Liquid Separation (J. Gregory, Ed.), Ellis Harwood, Chichester (1984) 172-182.

3- Gregory, J., *Chemical Engineering Sci.*, 36, 11 (1981) 1789-1794.

4- Gregory, J., *J. Colloid Interface Sci.*, 105, 2 (1985) 357-371.

5- Gregory, J., *Colloids Surfaces*, 31 (1988) 231-253.

6- Lapčik, L., Alince, B., van de Ven, T.G.M., *J. Pulp Pap. Sci.*, 21, 1 (1995) J19-J24.

7- Tam Doo, P.A., Kerekes, R.J., Pelton, R.H., *Private communication (1983).*

8- van de Ven, T.G.M., Alince, B., *J. Colloid Interface Sci.*, (in press).

9- Lindström, T., Glad-Nordmark, G., *Svensk Paperstidn.*, 15, (1978), 489-492.

10- Suurnäkki, A., Heijnesson, A., Buchert, J., Viikari, L., Westermark, U., *J. Pulp Pap. Sci.*, 22, 2 (1996) J43-J47.

11- Picaro, T., van de Ven, T.G.M., *J. Pulp Pap. Sci.*, 21, 1 (1995) J13-J18.

12- Rubio, J., *Colloids Surfaces*, 3, (1981), 79-95.

13- van de Ven, T.G.M., Alince, B., *J. Pulp Paper Sci.*, (in press).

14- Couture, L., van de Ven, T.G.M., *Colloids Surfaces*, 54 (1991) 245-260.

15- LaMer, V.K., Healy, T.W., *Rev. Pure Appl. Chem.*, 13 (1967) 112.

16- Takase, H., van de Ven, T.G.M., *Colloids Surfaces*, A, (to appear).

17- Stack, K.R., Dunn, L.A., Roberts, N.K., *J. Wood Chem. Tech.*, 13, 2 (1993) 283-308.

CHAPTER IV

GENERAL CONCLUSION AND SUMMARY

General conclusion and summary

The effects of three cofactors, sodium naphthalene sulphonate (SNS), modified phenolic resin (MPR), and carbamide (CAR), on a polyethylene oxide of a molecular weight of $7 \cdot 10^6$ were studied with the use of Dynamic Light Scattering (DLS) and Photometric Dispersion Analyser (PDA).

DLS of polymer solutions revealed that the polymer free coil diameter was in agreement with the literature, 129 nm for a freshly filtered solution and 72 nm for a solution containing clusters. Addition of each of the three cofactors to PEO solutions was found to create complexes: SNS did not change the apparent diameter significantly; CAR radically increased it; and MPR seems to decrease the size of the PEO chains.

The latex suspensions were also studied by DLS to elucidate the behaviour of the cofactors. In all experiments, CAR has shown deactivation of the latex particles for PEO. The SNS has been found very efficient in the sequence latex-polymer-cofactor (LPC), in increasing the PEO HLT. A thermodynamic equilibrium seems to take place at a HLT of about 40 nm. The mechanism by which the HLT is decreasing is thought to be due to a competitive adsorption between the cofactor molecules and the PEO chains, or a rearrangement of the PEO/SNS complexes and clusters at the surface of the latex. The MPR is the more efficient cofactor, in agreement with findings in literature. This is also the one from which the greatest difference in HLT with time was found. Because of the shrinking of PEO apparent diameter, rearrangement and flattening of the PEO chains is though to be the cause of the decrease in HLT.

The use of PDA provided information on the flocculation kinetics of wood fines. UV-spectroscopy revealed that SNS adsorbs onto the fines whereas MPR does not.

Flocculation experiments with PEO only (no cofactor) suggested that the fines are composed of more than one component, and asymmetric heteroflocculation was proposed as the flocculation mechanism. A model of fully lignin-coated and pure cellulose fines is proposed to explain the situation.

Addition of CAR with PEO did not enhance the flocculation of fines. CAR was found to create complexes with PEO in chapter II. Hydrogen bonding is thought to be operative between a PEO and a CAR molecule. However this seems to not be sufficient to flocculate a pulp suspension, and other compounds containing phenolic groups like SNS and MPR are a lot more efficient.

SNS was found to make all the fines alike by adsorbing on them. Adding the PEO after SNS gave homoflocculation, where half coverage was assumed to happen at the fastest flocculation rate. The specific surface of fines, calculated by PEO adsorption was found to be 0.223 m^2/g. When PEO was added prior to SNS, a decrease in the detachment rate constant happened. The particles are thought to become more sticky with the addition of the cofactors. The same mechanism is proposed for MPR when added after the PEO. In the other sequence, fines-cofactor-polymer (FCP), the PEO might partially heteroflocculate the fines prior to its complexation with MPR (this cofactor does not adsorb onto bare fines). This hypothesis is based on the significantly large value of the ratio $t_{P\text{-}C} / t_{P\text{-}F}$, the time required for the cofactor molecules to adsorb on a fraction of the PEO molecules over the time required for the same fraction of PEO to adsorb onto the fines respectively.

The association-induced polymer bridging mechanism can happen in three different manners depending if the cofactor and the polymer are adsorbing onto fines. When neither of PEO nor cofactor adsorb onto the collector, the PEO/cofactor association-complexes bridge the particles (van de Ven and Alince (1996)). When the cofactor and the polymer adsorb onto the fines, in the sequence fines-cofactor-polymer (FCP), with a chemical ratio cofactor / PEO of 3 / 1, adsorption of the PEO chains onto cofactor-coated fines is likely to occur at the beginning followed by the flocculation of the fines. In the sequence fines-polymer-cofactor (FPC), when the polymer adsorbs onto the fines and the cofactor adsorbs or not, a reenforcement of the bondstrength was noticed. This could be caused by the bridging of PEO-coated fines by the cofactor.

In both cases of MPR and SNS, it is difficult to distinguish between the three mechanisms because of the fast flocculation kinetics, and one should consider all possibilities for any type of cofactor. As seen in the literature review and in this research, the behaviour of PEO is always varying depending on the type of cofactor used. Cofactors should always been studied regarding several aspects to discover their properties and the best way they should be applied in papermaking.

Recommendations for future work

It would have been interesting to try MPR in the sequence LPC in DLS experiments to confirm if its mechanism is different from the one of SNS. The pure polymer solution were also studied with the bimodal model. This work has not been finished and would be interesting to continue to determine the size of the PEO clusters of such a high molecular weight. From the same model, the determination of the size changes due to the addition of a cofactor might be possible. Another suggestion to find out the effect of the cofactor on the single PEO chains is to mix the two chemicals together and filter them through a 0.2 µm chromatographic filter. If measurements are taken immediately after filtration, it could be possible to see if the chains (no clusters) have increased or decreased in diameter.

APPENDIX I

PHOTON CORRELATION SPECTROSCOPY

1.0 THEORY

Colloidal particles or polymer molecules are in perpetual movement due to Brownian forces (Chapter I). Light scattering occurs when a light beam is directed to such a colloidal suspension. The average and variations in scattered intensity are characteristic of the suspended particles. In dynamic light scattering (DLS), the intensity fluctuations are studied rather then the averaged intensity. The fluctuation analysis gives an autocorrelation between I(t) and I(t-τ). When τ is large I(t) and I(t-τ) becomes independent while they are closely related if τ is small. The autocorrelation function is a measure of the probability of a particle moving a given distance in a time τ. The fluctuating intensity signal is converted to its characteristic autocorrelation function, which for homodyne detection is,

$$G^{(2)}(\tau)=\langle I(0)I(\tau)\rangle \tag{1}$$

This autocorrelation function for a monodisperse dispersion is given by,

$$G^{(2)}(\tau)=I^2(1+e^{-2\Gamma\tau}) \tag{2}$$

where I is the averaged amount of light reaching the detector per unit time,

$$I=\langle I(t)\rangle \tag{3}$$

and Γ is the linewith distribution defined as,

$$\Gamma=Dq^2 \tag{4}$$

where D is the diffusion coefficient and q is the scattering vector.

$$D = \frac{kT}{6\pi\eta a} \tag{5}$$

kT is the thermal energy, η is the viscosity and a is the particle radius. The scattering vector is defined as,

$$q = \frac{4\pi m_2}{\lambda_0} \sin\left(\frac{\theta}{2}\right) \tag{6}$$

where m_2 is the index of refraction of the suspending medium, λ_0 is the wavelength of the incident beam, and θ is the scattering angle.

The normalised homodyne autocorrelation for a monodisperse dispersion is,

$$g^{(2)}(\tau) = 1 + e^{-2\Gamma\tau} \tag{7}$$

For a bimodal colloidal dispersion, heterodyne detection gives an other autocorrelation,

$$G_{BI}^{(1)}(\tau) = I_A\ e^{(-\Gamma_A\tau)} + I_B\ e^{(-\Gamma_B\tau)} \tag{8}$$

where A and B are for smaller and bigger sizes respectively. In the presence of B » A and B is still moving following Brownian motion, The scattered intensity will follow quasi-heterodyning. Using the Siegert relationship we obtain,

$$g_{BI}^{(2)} = 1 + \frac{I_A^2}{(I_A+I_B)^2}\ e^{(-2\Gamma_A\tau)} + \frac{2I_AI_B}{(I_A+I_B)^2}\ e^{(-\Gamma_A\tau)}\ e^{(-\Gamma_B\tau)} + \frac{I_B^2}{(I_A+I_B)^2}\ e^{(-2\Gamma_B\tau)} \tag{9}$$

For a polydisperse dispersion the cumulant method is used,

$$G^{(1)}_{poly}(\tau) = \sum_{i=1}^{N} I_i \, e^{(-\Gamma_i \tau)} \qquad (10)$$

where the subscript I is for a given size of particles. The normalized equation is,

$$g^{(2)}(\tau) = 1 + e^{-2\Gamma\tau} \left(1 + \frac{1}{2}\mu_2\tau^2 - \frac{1}{6}\mu_3\tau^3 + \ldots\right)^2 \qquad (11)$$

where Γ is the average value of Γ.

2.0 INSTRUMENTATION

A Brookhaven BI-2030AT photon correlator/goniometer equipped with a 50 mW He-Ne laser ($\lambda_0 = 632.8$ nm) was used. The autocorrelation function in the BI-2030AT consists of 72 data channels each separated from the previous one by a time $\Delta\tau$, the sample time, which can be varied depending on the time scale of the experimental decay, Γ.

The actual measured homodyne autocorrelatiohn function for scattered light from a monodisperse colloidal dispersion is,

$$G^{(2)}(\tau) = B(1 + b\, e^{-2\Gamma\tau}) \qquad (12)$$

where B is the baseline which is given by,

$$B = \frac{I_T^2}{16\, N_s} \qquad (13)$$

and the total intensity for one experiment is given by,

$$I_T = I\ Dur \qquad (14)$$

where Dur is the duration of one experiment. N_s is the number of samples in one experiment,

$$N_s = \frac{Dur}{\Delta\tau} \tag{15}$$

where $\Delta\tau$ is often referred as the sample time.

Figure 1 depicts the global view of the apparatus whereas Figure 2 is a closer view of the goniometer.

Figure 1: View of the BI-2030AT photon correlator/goniometer, comprising the correlator (1), the AT (80-286 processor) computer (2), the XT (80-86 processor) computer (3), the printer (4), the He-Ne laser (5), and the goniometer (6). The original AT-computer (2) controls the correlator. The XT-computer (3) controls the AT-computer and offers advantages of the use of homemade programs.

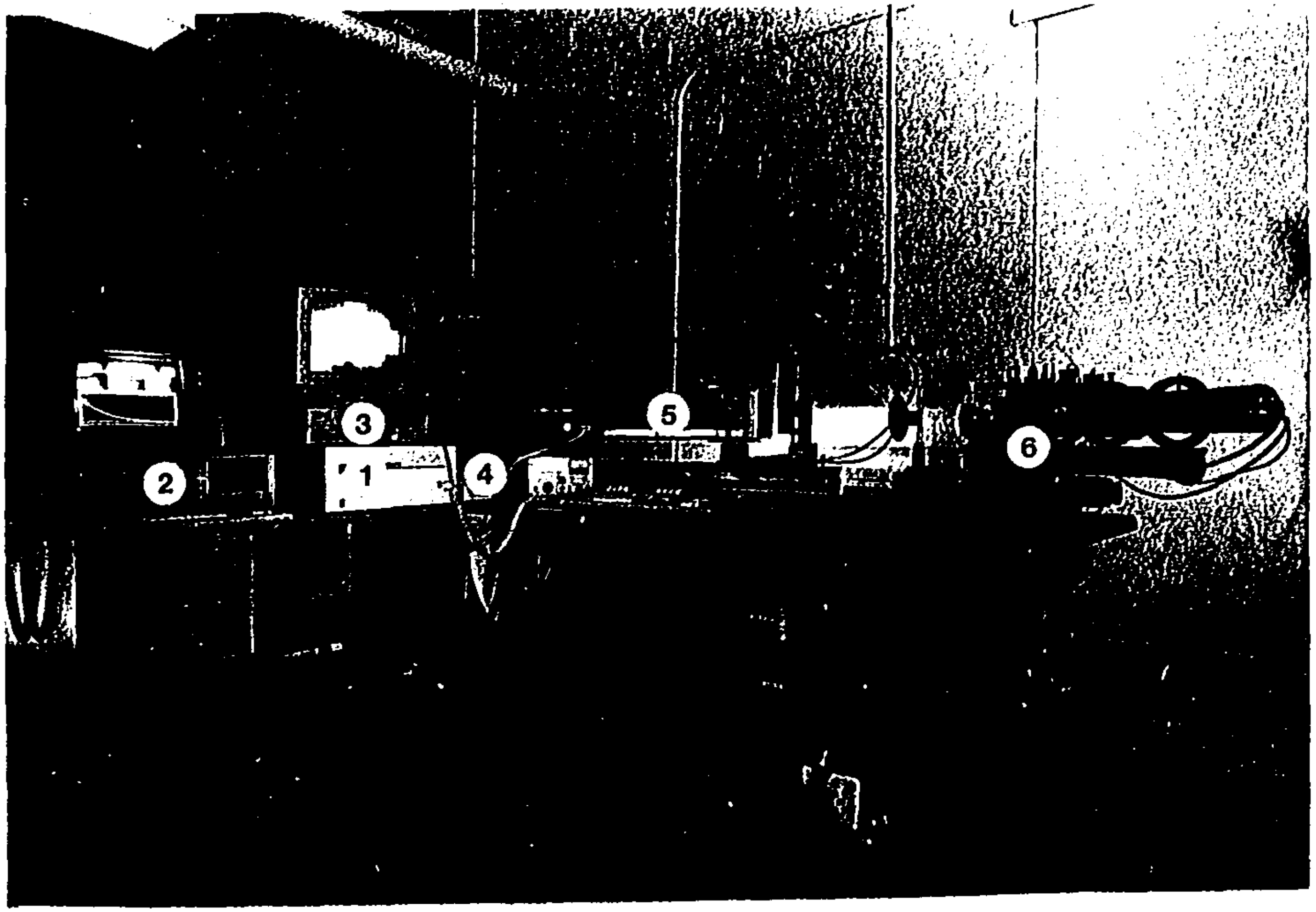
2
3
1
4
5
6

Figure 2: View of the goniometer. The samples to be impinged by the light beam are introduced in the cell assembly (1). The photomultiplier tube and its optics (2) can be moved at different angles from the beam trajectory. Two set of apertures (3 and 4) are used to adjust the light intensity. The cell assembly was kept at a constant temperature with a temperature controller (5). A peristaltic pump (6) was used to filter the index-matching liquid surrounding the sample cell.

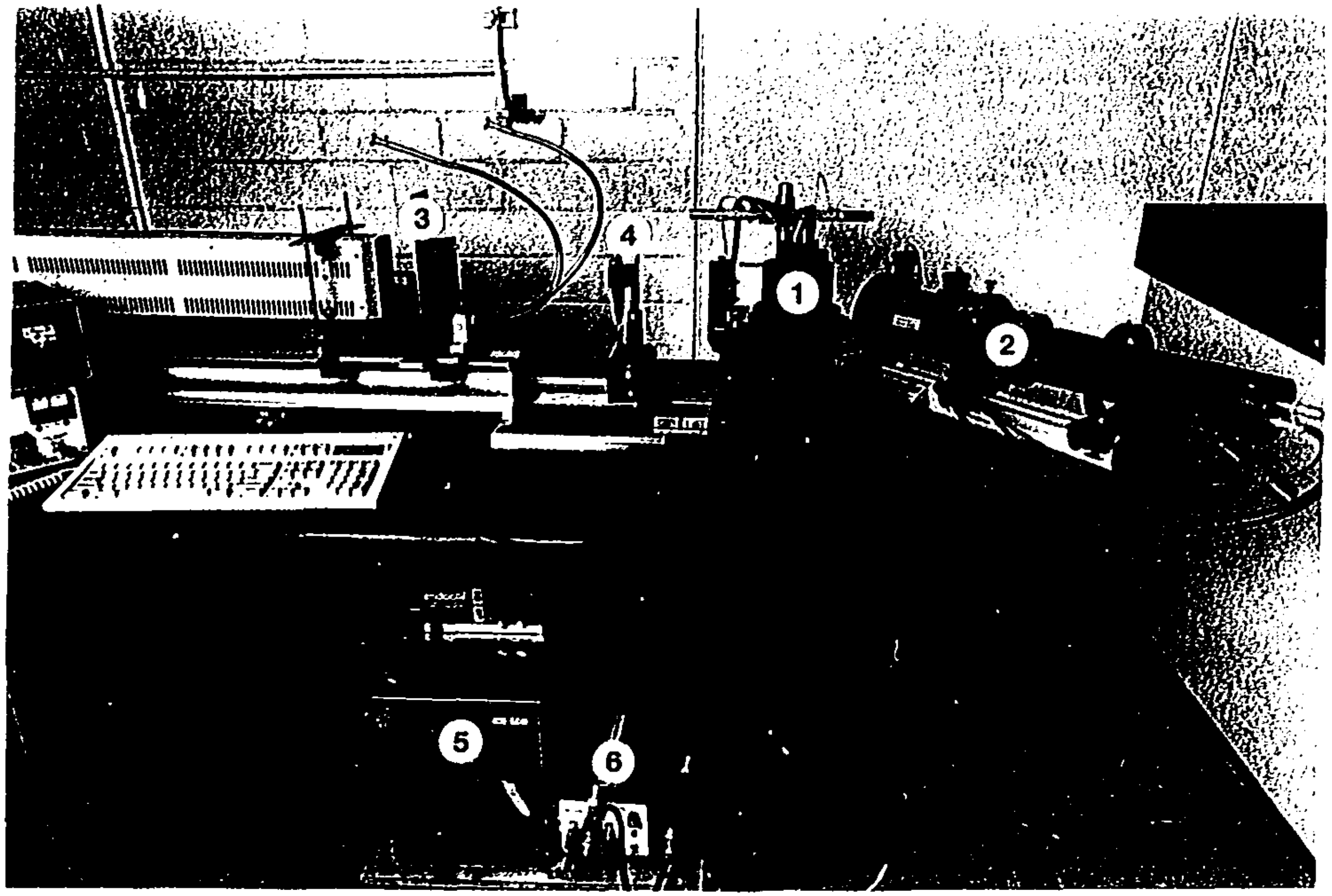
3
4
1
2
5
6